Submitted to Critical Reviews
in Environmental Control

LBL-6169
Preprint

RADIOLOGICAL ENVIRONMENTAL IMPACT OF HIGH-ENERGY ACCELERATORS

Ralph H. Thomas and Allessandro Rindi

February 1979

Prepared for the U. S. Department of Energy
under Contract W-7405-ENG-48

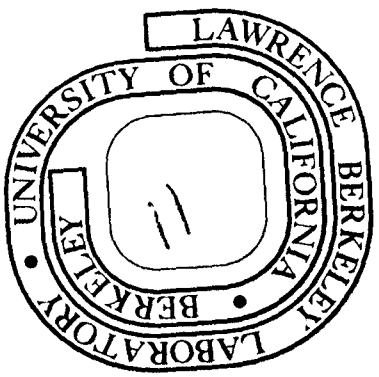

DISCLAIMER

RADIOLOGICAL ENVIRONMENTAL IMPACT OF HIGH-ENERGY ACCELERATORS

Authors: **Ralph H. Thomas**
Health Physics Department
Lawrence Berkeley Laboratory
University of California
Berkeley, California

Allessandro Rindi
University of Pisa
Pisa, Italy

Referees: Andrew P. Hull
William Robert Casey
Safety and Environmental Protection Division
Brookhaven National Laboratory
Upton, New York

And, as imagination bodies forth
The form of things unknown, the poet's pen
Turns them to shapes, and gives to airy nothing
A local habitation and a name.
Such tricks hath strong imagination,
. . .
And in the night, imagining some fear
How easy is a bush suppos'd a bear!

W. Shakespeare
A Midsummer Night's Dream. V.i.7

I. INTRODUCTION

High-energy accelerators are large facilities, in some cases occupying an area of a few square miles.* Since such projects are federally funded and may involve significant environmental effects, an environmental impact statement is required for any new high-energy accelerator in the U.S.[1]

It is certainly good health physics practice that possible radiological impacts of any new accelerator be studied. Such a study is greatly assisted by the considerable amount of experience with a variety of large accelerators over the past 30 years. It is most important to place the

* Space does not permit any discussion of particle accelerators in this review. The interested reader is referred to texts such as *Particle Accelerators* by M. S. Livingston and J. P. Blewitt. In this review, the term "high energy" is arbitrarily taken to be 1 GeV (10^9 eV).

radiological impact of accelerators in perspective, since it is usually minor when compared with other environmental impacts such as changes in land utilization, inconvenience during the construction period, water and electrical consumption, and visual impact.

High-energy accelerators are not generally regarded as potential sources of significant environmental radiation or radioactivity. Indeed, by comparison with nuclear reactors, they produce rather small quantities of radioactivity. For example, a large accelerator such as the 30-GeV proton synchrotron at the Brookhaven National Laboratory can only produce a maximum inventory of ~5000 Ci of radionuclides (most of which are short lived) compared to an inventory of ~5000 MCi per year in the case of a 1000-MW water power reactor.[2] Nevertheless, as we shall see, the quantities of radionuclides produced directly in the environment by accelerators can be comparable with the quantities of radionuclides released to the environment by some power reactors.

High-energy accelerators are potent local radiation sources and need to be heavily shielded for radiation safety and to facilitate their experimental utilization. Depending on the size of the accelerator and the cost of excavation of the construction site, there are two solutions to the external shielding problem.

The first solution is to build the accelerator at the ground surface level and contain within a permanent or demountable concrete vault. Additional earth shielding may then be added if needed. With such a shielding arrangement, prompt radiation is the dominant radiological impact because of the necessary limitations on the thickness of the shielding. The Bevatron at the Lawrence Berkeley Laboratory (Figure 1), NIMROD at the Rutherford Laboratory, the 28-GeV proton synchrotron (Figure 2), and the 600-MeV Synchrocyclotron at the European Center for Nuclear Research (CERN) are examples of accelerators built at ground level and surrounded by concrete and earth shielding. Figure 1 shows a typical concrete block shielding construction. Figure 3 shows the 2-mile Stanford Linear Accelerator which was built using cut and cover earth-moving techniques.

The second solution consists of burying the

A

FIGURE 1. Three successive phases of the construction of the shielding around the Bevatron at the Lawrence Berkeley Laboratory (early 1963).

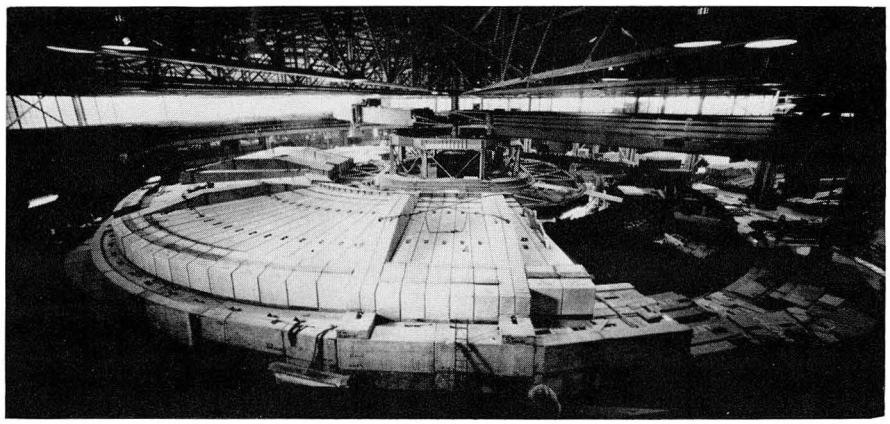

FIGURE 1B

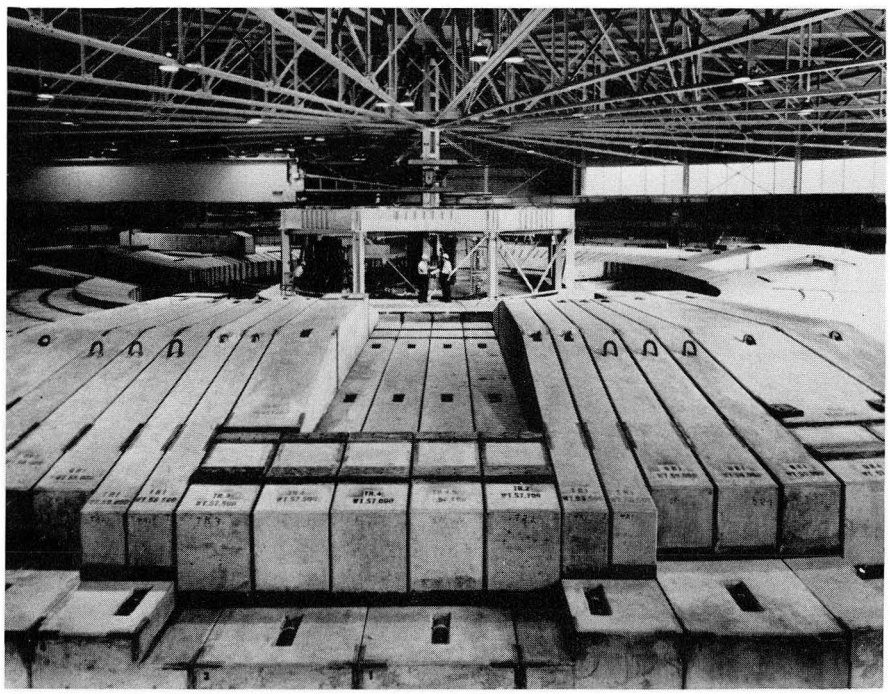

FIGURE 1C

accelerator underground to provide economical radiation shielding. An example of such an underground accelerator is the CERN 400-GeV proton synchrocyclotron (Figure 4). In addition to the cost of excavating or tunnelling, this solution has the following disadvantages:

1. A certain amount of radiation may still penetrate the containment.
2. It is usually difficult or very expensive to locate the experimental areas underground, and one is forced to bring particle beams to the surface restoring the shielding problem to ground level.
3. The particle flux densities generated in the earth and ground water may be sufficiently large so that radioactivity could appear in the local ground-water systems.

To give some feeling for magnitude, it should

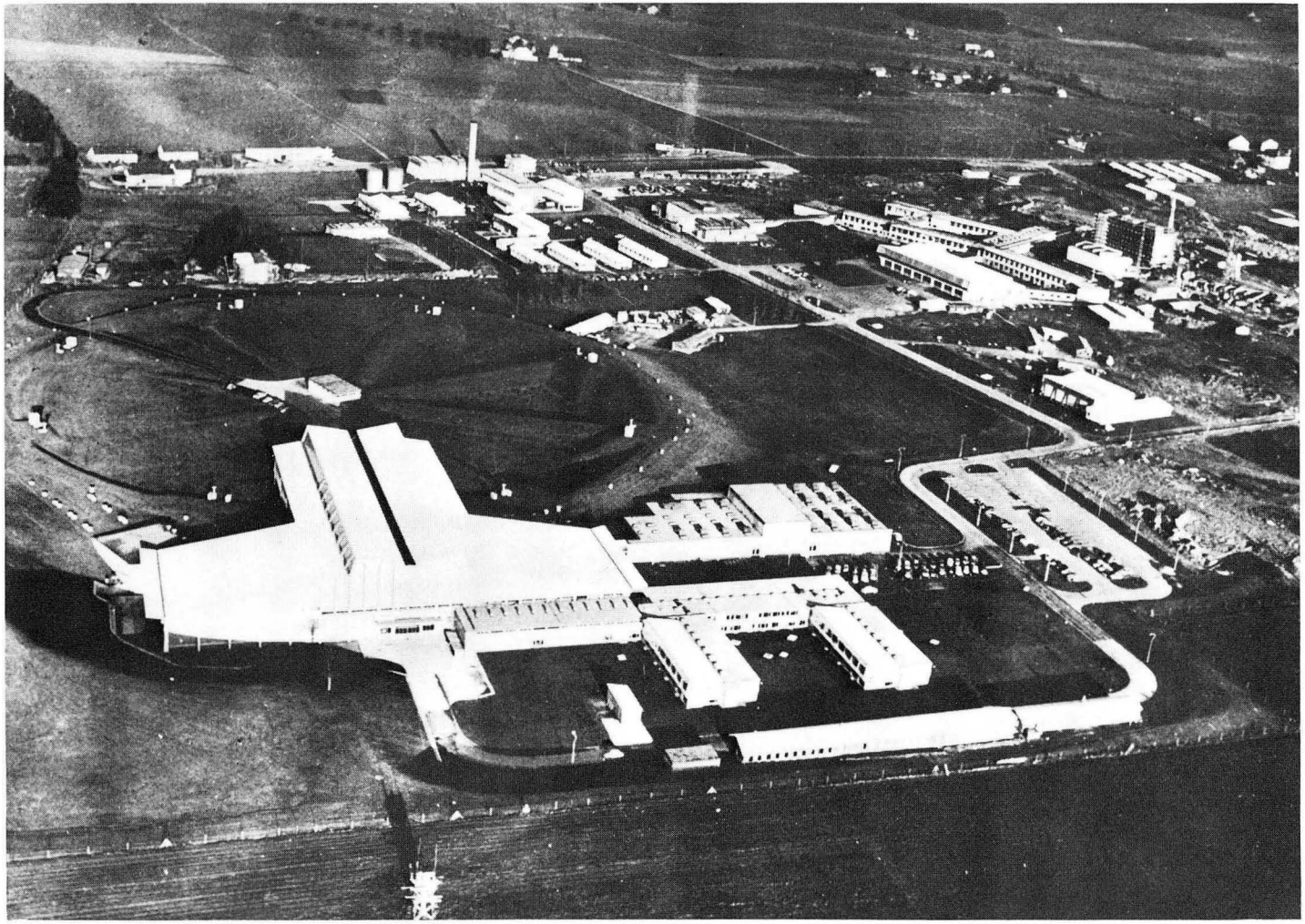

FIGURE 2. The 28-GeV proton synchrotron at CERN in Geneva. The accelerator is built at ground level and contained in a concrete vault covered by earth.

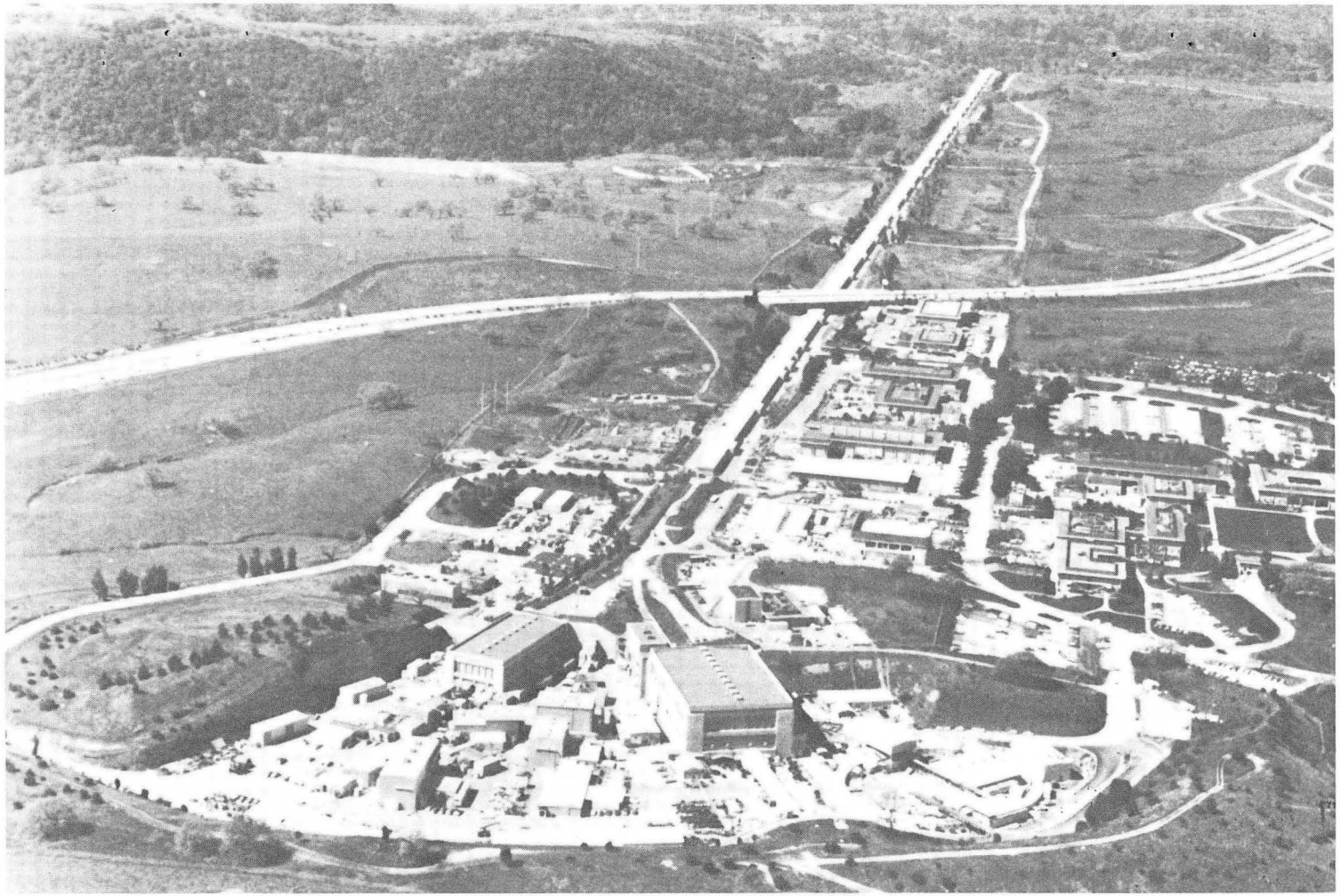

FIGURE 3. The 20-GeV electron linac at Stanford. The accelerator was built using cut and cover earth-moving techniques. The klystron gallery can be seen at the present grade level. The accelerator structure is buried 30 ft below the ground surface.

FIGURE 4. A. The CERN 400-GeV proton synchrotron tunnel under construction. B. The completed tunnel. C. An aerial view of the accelerator site showing the undisturbed ground surface.

be noted that a continuous flux density of $\sim 10^5$ neutrons per square centimeter per second of high-energy particles will produce, at equilibrium, a tritium concentration of 2 μCi/l in water — corresponding to 2% of the maximum permissible concentration in drinking water for radiation workers.[3] At CERN, the maximum high-energy flux density observed in the earth shield is $\sim 10^6$ neutrons per square centimeter per second.[4] The total inventory of tritium produced in the shields of the new generation of high-energy accelerators is on the order of tens of curies at saturation.[5] This quantity is produced directly in the environment and thus, under certain conditions, might be considered a release comparable to or in excess of that re-

FIGURE 4B

ported for many power reactors.[6] Thus, for accelerators buried underground, in addition to prompt radiation, the possible contamination of ground-water systems should be investigated.

In addition to these two factors, it may also be necessary to consider two other influences on the environment. Irradiation of the air in accelerator buildings will produce both radionuclides and toxic chemicals such as ozone and oxides of nitrogen. Normal air changes will transport these radiation products to the environment. A second potential radiological impact arises from possible radioactive contamination of the environment following the recycling of materials used in accelerator construction. Little attention has been given to this possible source of contamination because at the present time it is minimal. Few radioactive accelerator components are recycled but, as the number of decommissioned accelerators grows, economic pressures will require that careful study of this potential problem be made. Due to lack of published data, this topic is not considered in this review.

In the past few years, considerable information has been published describing the environmental surveillance programs of laboratories operating large accelerators. Of great value in this respect are the environmental monitoring reports of U.S. Atomic Energy Commission-(USAEC) operated facilities which have been issued since 1961. Since 1972, compendia have been published which are an important source of data for intercomparison between different types of nuclear facilities.[7-9]

Studies of the environmental monitoring reports of multidisciplinary research laboratories

FIGURE 4C

with many diverse potential sources of radiological impact on the environment, such as Argonne National Laboratory, Brookhaven National Laboratory, or the Los Alamos Scientific Laboratory, show that accelerators have, in general, a relatively small impact. For example, at Brookhaven during 1974, the contribution from accelerator operations was only 0.7% of the total population dose equivalent due to all operations[10] (Table 1).

TABLE 1

Population Dose Equivalent (Brookhaven National Laboratory — 1974)

Airborne effluents	6.70 man rem
Liquid effluents	0.49 man rem
Forest γ-source	0.10 man rem
AGS skyshine	0.05 man rem
Total	7.34 man rem

In summary, the four possible radiological environmental impacts due to high-energy accelerators, in order of apparent importance are

1. The production of "prompt"* radiation fields during accelerator operation
2. The production of radionuclides and noxious chemicals (such as ozone and nitric oxide) in the air in the accelerator vault and their subsequent release
3. The production of radionuclides in the soil and ground water near the accelerator, with the possibility of infiltration in the underlying ground water systems and subsequent migration from the accelerator site into wells or other sources of potable water.
4. The induction of long-lived radionuclides in accelerator components which may subsequently be "recycled" with the consequent transmission of radionuclides into the general environment; this would be particularly true in the case of valuable metals such as copper, brass, iron, or aluminum

Thus, we see that the environmental impact of high-energy accelerators is different in character from most types of nuclear installations. As will be seen with accelerators, the predominant source of population exposure is due to the radiation field produced during operation rather than due to the leakage of radionuclides into the environment.

It is only in the past 5 or 6 years that the relative importance of radiological impact has been placed in this order. For many years, it was believed that the production of radionuclides in the soil and ground water would be the second most important source of impact. The fact that we now understand that the potential for radioactive contamination of ground water is very small is an important step forward in our understanding of accelerator-produced radiation. Accordingly, we discuss this question in some detail in this review.

II. THE PROMPT RADIATION ENVIRONMENT OF HIGH-ENERGY ACCELERATORS

A. The Production and Transport of Prompt Radiation

Extensive experience at both high-energy electron and proton accelerators have shown that, outside thick shielding, neutrons are usually the dominant source of dose equivalent.[11,12] However, at energies exceeding 10 GeV, muons can under certain circumstances, produce the largest contribution to dose equivalent.[13]

It may be surprising to some readers to learn that the radiation environments outside well-shielded electron accelerators are dominated by neutrons. The basic theoretical reasons for this observation have been given first by de Staebler[14] and later by Nelson and Jenkins.[12] A convincing demonstration of these theoretical principles is shown in Figure 5, where the variation with time of photon and neutron dose equivalent rates at the boundary of the Stanford Linear Accelerator Center (SLAC) is shown.[15] Operation of the SLAC 20-GeV electron linear accelerator has been observed to result in a radiation environment dominated by neutrons. Measurements of the neutron spectra outside thick shielding at the SLAC 20-GeV electron linac and the Bevatron (a 6-GeV proton synchrotron) have demonstrated similarities be-

* The word "prompt" is used to indicate that the radiation field exists only when the accelerator is operating.

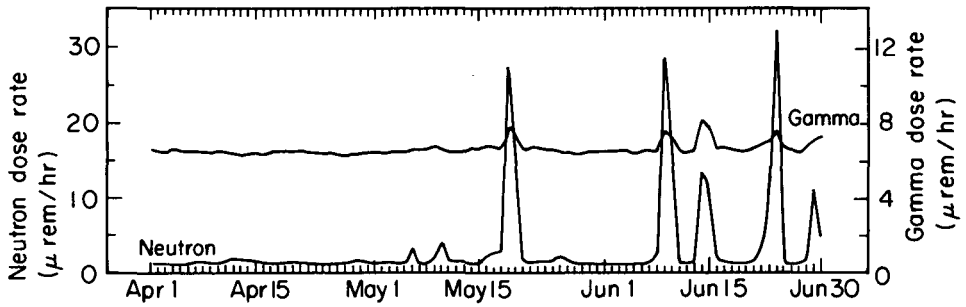

FIGURE 5. Quarterly dose equivalent rate plot recorded at a monitoring station located at the Stanford Linear Accelerator Center.

tween the environmental neutron spectra at both accelerators.[16]

A high-energy accelerator is a neutron source of considerable intensity. (For example, $\sim 10^9$ neutrons per second leak from the roof shielding of the Bevatron when it accelerates $\sim 10^{12}$ protons per second. A source strength of this magnitude will produce, at a distance of 1 km from the accelerator, a neutron flux density equal to the cosmic ray produced neutron background.[17])

Therefore, environmental surveillance programs at high-energy laboratories are usually largely devoted to neutron monitoring. Several descriptions of such monitoring programs have been published.[7,8,9,17-24]

Bonifas et al.[21] have described a convenient technique for measuring both the gamma-ray and neutron radiation levels around accelerators using thermoluminescent dosimeters. This method of measurement has the convenience of being relatively simple and inexpensive and may be used to determine the relative environmental impact of several large radiation sources which operate simultaneously — as is often the case at high-energy physics laboratories.

Figure 6 shows contours of equal neutron dose equivalent around the CERN laboratory site obtained by this technique. Four principal sources of radiation may be seen: the proton synchrotron (PS), synchrocyclotron (SC), the intersecting storage rings (ISR), and an experimental hall where a bubble chamber is installed. Radiation levels of 100mrem/year due to neutrons may be seen to exist at about 500 m from the proton synchrotron. As expected, the photon dose equivalent is roughly a factor of ten lower than that due to neutrons. With measurable radiation levels produced so far from high-energy accelerators, it is necessary to understand the transport of accelerator-produced neutrons to large distances to be able to estimate population exposures.

In recent years, some crude measurements have been made of the energy spectrum of the neutrons leaking from accelerator shielding and the influence of the shield material on this leakage spectrum.[25] The character of the shield-leakage neutron spectrum is controlled by the interaction of neutrons of energy greater than about 100 MeV. The nature of the equilibrium achieved between these high-energy neutrons and their interaction products is determined by the nuclear properties of the shield. Typically, neutrons contribute more than 90% of the total dose equivalent, and 50% of the neutron dose equivalent is contributed by neutrons with energies between 0.1 and 20 MeV. However, for certain leakage spectra, neutrons in the keV energy region (e.g., for steel shields) or neutrons above 20 MeV (for wet earth shields) may be more important than this general rule implies.[25] Changes in the leakage spectrum at the air interface are important in the transport of neutrons to large distances. When neutrons leave the shield, small changes in the spectrum — most noticeably in the neutron resonance region — are initiated. An equilibrium determined by the nuclear properties of air will be reestablished after passage through two to three interactions mean free paths, corresponding to several hundred meters in air.

Despite the lack of precise experimental data and the absence of an adequate theoretical study, neutron skyshine* phenomena at high-energy accelerators are empirically

* For a discussion of the definition of the term skyshine, see Reference 27.

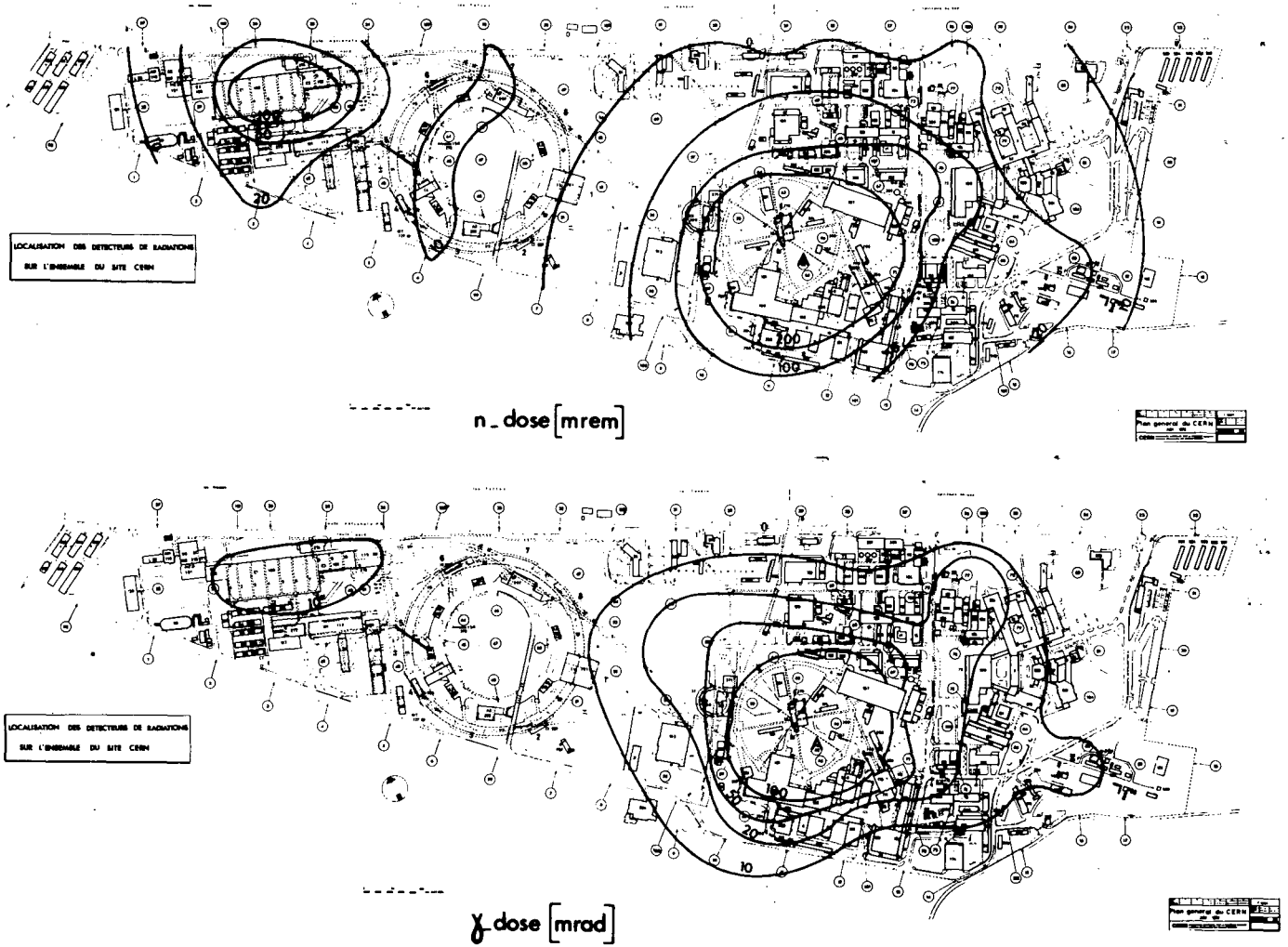

FIGURE 6. Contours of equal neutron dose equivalent at the CERN laboratory site. The set of contours to the left of each plan are centered around the 660-MeV synchro-cyclotron (SC). The central contour (upper plan only) crosses the intersecting storage rings (ISR). To the right of the plans are contours around the 28 GeV synchro-cyclotron (CPS). The radius of the CPS is 100 m and its center is just above the point "A" on the plans. Contours are in millirems (neutrons) and millirads (gammas).

understood.[26] Provided that an estimate of the source strength can be obtained, radiation levels up to distances of several hundred meters may be estimated to within a factor of about three. This is usually adequate for radiation-protection purposes. However, at the present time, there is no generally accepted formulation for skyshine phenomena. Jenkins[15] has discussed in some detail our inability to discriminate between alternative theoretical and empirical formalisms.

Jenkins[15] has suggested a variation of neutron dose equivalent with distance given by:

$$H(r) \propto \frac{e^{-r/\lambda}}{r} \quad (1)$$

where $\lambda = 140$ m.

At the Alternating Gradient Synchrotron of Brookhaven National Laboratory, an expression of the form:

$$H(r) \propto \frac{1}{r^2} \exp -(r - 854)/600 \quad (2)$$

where $r \geqslant 1000$ m is used,[30] with r measured in meters.

At CERN an expression of the form:

$$H(r) \propto \frac{1}{r^2} \exp(-r/640) \quad (3)$$

where r is measured in meters is used.[22]

More precise experimental studies of the transport of high-energy neutrons, particularly at distances beyond 2500 m from accelerators, and neutron spectrum measurements will be helpful in improving estimates of population dose equivalent.

Rindi and Thomas[27] have reviewed the published measurements of neutrons at large distances from high-energy accelerators. Figure 7 shows measurements of neutron flux density vs. distance made at six different accelerators. The authors were able to conclude from these and other data that despite difficulties in interpretation, the available experiment data are consistent with our present understanding of electromagnetic and hadron cascade phenomena and that:

1. The radiation intensity decreases at least as fast as the inverse of the square of the distance from the source.
2. At large distances from accelerators, neutrons are the dominant component of the radiation field.
3. For well-shielded accelerators in the GeV region, the neutron spectrum emerging

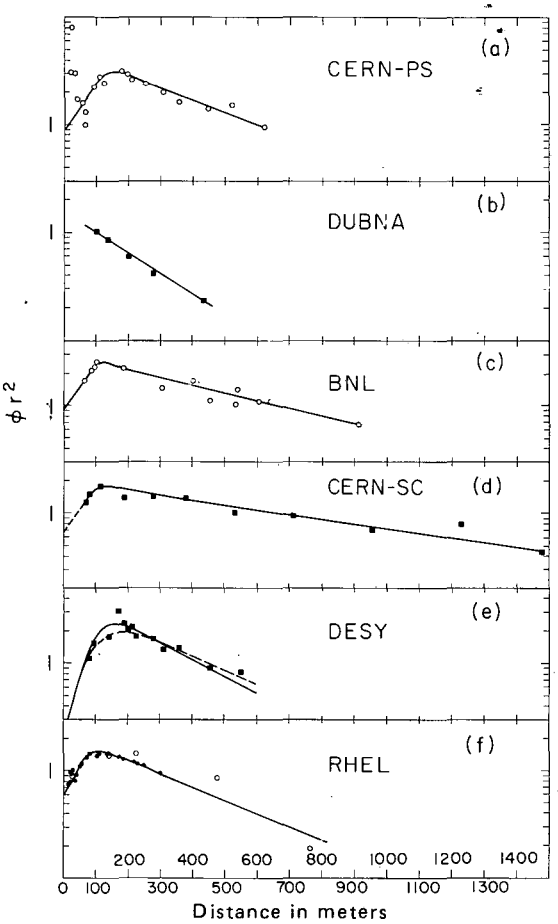

FIGURE 7. Measurements performed around different accelerators. The abscissa is the distance from the accelerator in meters, the ordinate is the product of the measured neutron flux density by the square of the distance. In these coordinates a $1/r^2$ variation shows up as a horizontal line. (a) Measurements of fast neutron flux density performed at the CERN 28-GeV Proton Synchro-cyclotron.[28] (b) Measurements of fast neutron flux density performed at the Dubna 10-GeV Proton Sychrophasotron.[29] (c) Measurements of dose-equivalent rate performed at the Brookhaven 30-GeV Proton AGS.[30] (d) Measurements of fast neutron flux density performed at the CERN 600-MeV Proton Synchro-cyclotron.[31] (e) Fast neutron flux density measurements performed at the DESY 7.5-GeV Electron Synchrotron.[32] (f) Fast neutron flux density measurements performed at the Rutherford Laboratory Proton Linear Accelerator: the solid dots indicate the measurements taken for a proton beam of 30 MeV,[33] and the open dots for a proton beam of 50 MeV.[34]

from the shield is in equilibrium. At lower energies or at accelerators with inadequate overhead shielding, hardening of the spectrum with distances is observed.

4. The empirical relation:

$$\phi_n(r) \approx \frac{a\ Q\ e^{-r/\lambda}}{4\pi r^2} \quad (4)$$

is a simple but adequate expression for the skyshine intensity around most accelerators where r is the distance from the accelerator, a is a constant that expresses the change in neutron spectrum that occurs in the transition from shield to air, and Q is the effective source strength of neutrons emitted from the shield surface. λ is the attenuation length of neutrons in air and values reported in the literature vary between 267 and 990 m. At large distances (several thousand meters — from our understanding of high-energy hadron cascades), we would expect λ to approach the value of $\sim$100 g cm^{-2}.

Little data have been reported in the literature since the review by Rindi and Thomas, which is therefore essentially up-to-date and the interested reader is referred to this article for a detailed discussion of the "prompt" radiation field of accelerators. However, Nakamura and colleagues have reported some new measurements of skyshine neutrons and photons produced by 52-MeV protons at the cyclotron of the Institute of Nuclear Study, Tokyo.[35] The measurements of accelerator produced skyshine photons are particularly interesting because they are the first such measurement reported in the literature.

The authors showed that skyshine photons are transported in the atmosphere with approximately the same dependence on distance as both thermal and fast neutrons. (These measurements support the hypothesis that the relative importance of photons will not increase with distance from high-energy accelerators. In fact at accelerators where photons are initially dominant, the fraction of total dose equivalent contributed by neutrons will increase because photons will be absorbed more rapidly in the atmosphere. Ultimately, an equilibrium will be achieved with high-energy neutrons controlling the photon production.) Measurements of the energy spectrum of scattered photons show a prominent 2.2-MeV peak due to the capture of thermal neutrons in hydrogen. At higher energies, the photon spectrum falls monotonically with a "knee" at about 7 MeV (see Figure 8).

Under certain shielding conditions, muons may be observed as a major component of the stray radiation field at the Brookhaven Alternating Gradient Synchrotron (AGS)[36] or the CERN Proton Synchrotron (PS).[37] Baarli and Hofert[37] have described the use of a counter telescope to locate the source of muons and leakage in the shielding at the CERN PS.

At the 500-GeV proton synchrotron of the Fermi National Accelerator Laboratory (FNAL), muons are the dominant component of the radiation level at the site boundary.[13] This is in part due to the large distances from the accelerator to the site boundary. Neutrons produced at the accelerator are greatly reduced in intensity by inverse square law and air attenuation at the laboratory perimeter. Muons, on the other hand, as a consequence of experimental use of the accelerator, are produced in a highly collimated beam directed towards the site boundary. Because of their weak interaction with matter, they survive thick shielding and emerge into the air still well collimated. At the site boundary, a well-defined "beam" $\sim$50 m wide can be identified.[13] The maximum dose equivalent at the site boundary was 2 mrem during 1974. Radiation levels outside this "beam" were at least a factor of ten lower. At FNAL, as at CERN, a muon telescope is used to locate the origin of the more energetic muons.

B. Population Exposure from High-energy Accelerator Prompt Radiation

Because the prompt radiation field dominates the radiation environment of high-energy accelerators, as we shall show, it is the dominant source of population exposure resulting from accelerator operations.

At the present time, there is no generally accepted method of calculating the population exposure resulting from accelerator operation because the precise form of the variation of dose equivalent with distance is not yet precisely known.[15,27] In the following discussion, a model suggested by Stephens et al.[38,39] is described.

The population dose equivalent resulting

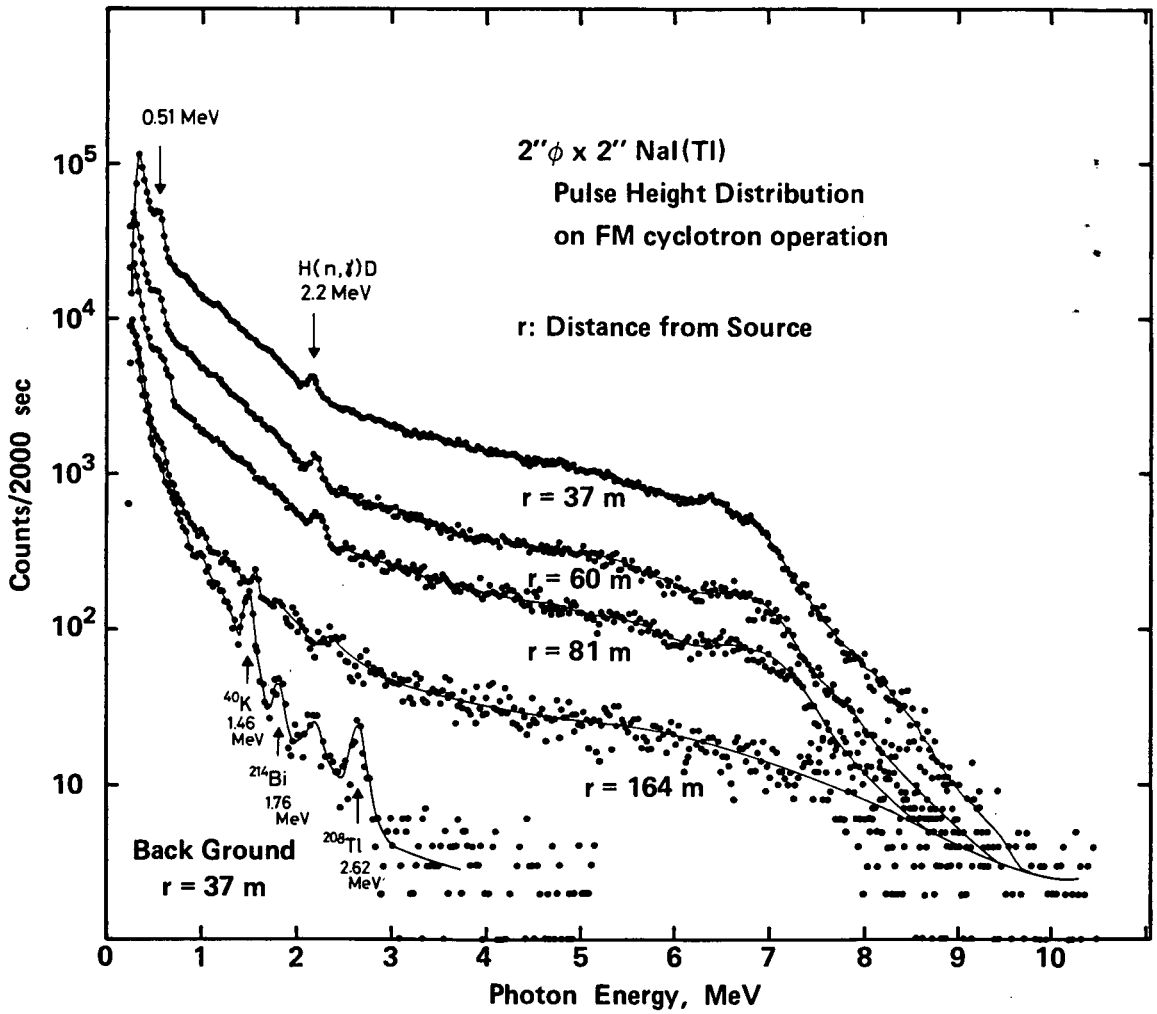

FIGURE 8. Spectra of skyshine photons taken at different distances from a 52-MeV proton cyclotron.[35]

from operation of a nuclear facility, M, is defined by the equation:[40]

$$M = \int_{H_{MIN}}^{H_{MAX}} H\,N(H)\,dH \qquad (5)$$

where N(H)dH is the number of people receiving a dose equivalent (H), and the subscripts refer to the minimum and maximum dose equivalent.

For accelerator laboratories, where M is averaged over an extended period such as a year, it has been suggested that[38] Equation 5 be replaced by the equation:

$$M = \int_{R_{MIN}}^{R_{MAX}} H(r)\,N(r)\,dr \qquad (6)$$

where H(r) is the annual dose equivalent at a distance r from the accelerator, and R_{MAX} and R_{MIN} are the furthest and closest possible distance within which members of the public approach the accelerator.

It has been shown[39] that Equation 6 may be numerically evaluated using the approximation:

$$M = \frac{2\pi r_0^2 \, H_0 \, e^{r_0/\lambda}}{S_1 S_2} \sum_{i=0}^{i=n} \frac{N_i}{\pi (r_i^2 - r_{i-1}^2)} \int_{r_{i-1}}^{r_i} \frac{e^{-r/\lambda}}{r} \, dr \qquad (7)$$

where H_o is the annual dose equivalent at the Laboratory boundary; λ has previously been defined (Section II.A); N_i is the average number of people who may be considered permanently resident between distances r_{i-1} and r_i from the accelerator; S_1, S_2 are shielding factors for surrounding hills and buildings; and r_0, r_n correspond to R_{MIN} and R_{MAX} in Equation 6.

The accuracy of the estimate of population dose equivalent obtained using Equation 7 will depend upon whether the parameters λ and n are correctly chosen.

λ may take values in the range from about 225 m (corresponding to a fission spectrum) to 850 m (corresponding to neutrons with energy greater than 100 MeV).[27] Assuming a uniform population density around an accelerator laboratory, Stephens et al.[38] showed that the population dose equivalent was approximately proportional to $\lambda^{2/3}$. Thus, if a conservative value of λ is assumed (850 m), the population dose equivalent could be overestimated by as much as a factor of 2.5 if the leakage spectrum from the accelerator shield were rich in low-energy neutrons.

Typically, the population dose equivalent converges towards its ultimate value within a few kilometers from the accelerator. For example, at the Lawrence Berkeley Laboratory (LBL), the population dose equivalent reaches its ultimate value at about 5 km from the laboratory (Figure 9). Thus, although it is conventional to quote the 80-km (50 mile) population dose equivalent, the value of r_n in Equation 7 will, in general, be much smaller.

The extent of the radiological impact on the environment due to penetrating radiation produced by high-energy accelerators may be measured by the parameter M/H_0 (population dose equivalent per unit fence post dose equivalent).

At LBL, numerical integration gave M/H_0 = 1023 man rem per fence-post rem.[38] This value probably represents an upper limit to the value of M/H_0 likely to be found at accelerator laboratories, since the LBL is situated adjacent to fairly densely populated areas of the San Francisco Bay Region.*[17] About 170,000 people live within 5 km of the laboratory, at an average population density ranging from 2000 to 3000 persons per square kilometer.

In calculating the population dose equivalent due to operations at the Stanford Linear Accelerator Center, the variation of dose equivalent with distance is assumed to be of the form:[15]

$$H(r) \propto \frac{e^{-r/\lambda}}{r} \qquad (8)$$

where λ = 140 m, and a value of M/H_0 = 460 man rem per fence post rem was obtained.[42] This value is somewhat lower than that at the LBL for two reasons. First, the population density around the Stanford accelerator is somewhat lower than that at Berkeley, and second, the evaluation of dose equivalent was only carried out to a distance of 1 mile from the accelerator. Nevertheless, the population dose equivalent produced by these two centers which have similar locations — adjacent to a university campus and a large urban population — is seen to be comparable in magnitude.

At CERN, where the average population density around the laboratory is considerably lower than at Berkeley (see Table 2), M/H_0 has the value 160 man rem per fence post rem.[23]

At laboratories such as Brookhaven National Laboratory (BNL), where the site boundaries are at considerable distance from the accelerator-produced radiation sources, the parameter M/H_0 has a low value. At BNL, the value M/H_0, estimated from data contained in Environmental Report for 1975, is 54 man rem per fence post rem.[44]

At the Fermi National Accelerator Laboratory (FNAL), the population dose equivalent was largely due to penetrating muons which were directed towards the northeast boundary of the laboratory. Baker[45] has estimated a population dose equivalent of 1 man rem resulting from a total dose equivalent of 1 mrem during

* Recently, one of the authors visited the Institute for Nuclear Study, University of Tokyo. This laboratory is situated in suburban Tokyo where the population density is greater than that at Berkeley, and private homes are situated within 50 m from the laboratory's accelerator.

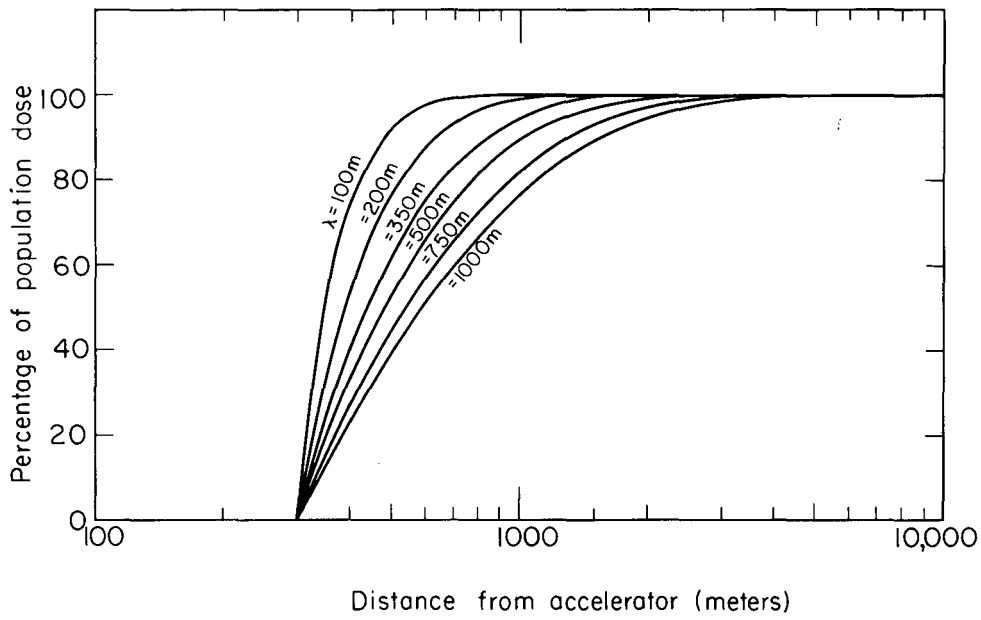

FIGURE 9. The convergence of the population dose equivalent as a function of distance from the accelerator for attenuation lengths for neutrons in air, λ, between 100 and 1000m.

TABLE 2

Summary of Population Dose Equivalent Estimates for Several High-energy Accelerators

Laboratory	M/H_0 (man rem per fence-post rem)	Comments	Ref.
Lawrence Berkeley Laboratory	1023	~170,000 people living within 5 km from the laboratory; Average population density 2—3 × 10^3 persons per square kilometer	39
Stanford Linear Accelerator Center	460	Population dose equivalent calculated out to 1 km from the laboratory	41, 42
CERN European Organization for Nuclear Research	160	30,000 people living within 4 km from the laboratory; population density 35 persons per square kilometer ≤1 km, 640 persons per square kilometer ≥1 km from laboratory	23, 43
Brookhaven National Laboratory	54	7,381 persons living within 5 km of the laboratory; 5.2 × 10^6 people living within 80 km of laboratory; population density of ~ 260 persons per square kilometer	44
Fermi National Accelerator	1000	Dose due to collimated muon beam ~ 50 m wide at site boundary; approximately 100,000 people in irradiated zone	45

1975 over a region about 50 m wide at the FNAL site boundary.

When the fence post dose equivalent due to accelerators is only a few millirems per year, spatial and secular variations in natural background place a limit on the accuracy to which the fence post dose equivalent, due to photons, and detector sensitivity may be determined. These problems have been discussed in detail elsewhere.[17,46,47]

III. INDUCED RADIOACTIVITY PRODUCED IN ACCELERATOR SHIELDS AND WATER IN THE GROUND

Particle accelerators are potential sources of large quantities of radioactivity. A rough estimate of the total quantity of radioactivity in curies produced by a proton accelerator at equilibrium Q_{SAT} may be obtained from the equation:[50]

$$Q_{SAT} \approx \frac{Bi}{3.7 \times 10^{10}} \text{ Ci} \qquad (9)$$

where is the proton intensity (protons per second) and B is a multiplication factor. For the alternating gradient synchrotron at the Brookhaven National Laboratory, B has a value of ~24[48] and thus:

$$Q_{SAT} \approx 6.5 \times 10^{-10} \text{ Ci per proton sec (at 30 GeV)} \qquad (10)$$

At an intensity of 5×10^{12} protons per second, Equation 10 predicts a saturation activity of 3250 Ci. It is reasonable to assume that the total activity will be directly proportional to the beam power and, thus, we finally obtain:

$$Q \approx 135 \text{ Ci/kW} \qquad (11)$$

for high-energy proton accelerators (E > 1 GeV).

By contrast, high-energy electron accelerators are less efficient in producing radioactivity by about a factor of 100.

Swanson[49] has estimated that at the Stanford 20 GeV electron linac, the total inventory of radioactivity in the accelerator structure is ~5 Ci. This quantity of radioactivity is produced by 2% of the total beam energy, which averages 200 kW. The quantity of radioactivity produced per kilowatt of beam power is then:

$$Q \approx 1.25 \text{ Ci/kW}$$

Most of the induced radioactivity will be produced in the accelerator structure and shield and is therefore tightly bound in the constituent materials and is not likely to migrate into the environment. However, several possible pathways do exist for the production of radionuclides in or transfer to the environment. In order of importance these are

1. The direct production of radionuclides in the earth and ground water surrounding the accelerator and their subsequent migration to the water table
2. The release of radioactive gases and aerosols, produced in the accelerator room, to the environment
3. The transfer to the environment of dust and metallic particles produced during accelerator maintenance

The first of these pathways will be discussed in this section, while the other two pathways will be discussed in Section IV.

A. Total Activity Produced in Earth Shield and Ground Water

It is of interest to first have some idea of the magnitude of the total activity produced by activation in the earth shield surrounding a high-energy accelerator.

Stapleton and Thomas[5] have suggested that the total quantity of radionuclides at saturation, Q, produced in the ground water in the shield of an accelerator buried underground is given by the empirical equation:

$$Q = 2\pi f \langle\sigma\rangle \frac{(\rho L)}{M} a \mu \lambda \phi_0 \text{ dis sec}^{-1} \qquad (13)$$

where f = fraction by weight of water in shield; ρ = shield density; L = Avogadro's number; M = molecular weight of water; $\langle\sigma\rangle$ = production cross-section averaged over the neutron spectrum; ϕ_0 = neutron flux density ($E > E_0$) at r = a, z = 0, where E_0 is the reaction threshold energy; a = effective radius of machine tunnel; λ = neutron flux relaxation length in transverse direction; and μ = neutron flux relaxation length in longitudinal direction.

Values of the parameters a, μ, λ, and ϕ_0 appearing in Equation 13 were determined in an experiment carried out at the CERN 28-GeV proton synchrotron.[4] This experiment also supports the assumption that the number of secondary particles generated in the earth shield is directly proportional to beam power. This

model may therefore be scaled to higher energy proton accelerators. Experience shows that the high-flux density regions in the accelerator are closely confined around the regions of interaction.

At proton energy of 25 GeV and for an intensity of 10^{12} protons per second, the values of the parameters of Equation 13 obtained by Gilbert et al.[4] were: a = 390 cm; μ = 650 cm; λ = 53 cm; ϱ_{earth} = 2.16 g cm^{-3}; f = 0.15 (fraction of water by weight in earth shield); and ϕ_0 (E > 20 MeV) = 6×10^5 particles cm^{-2}/sec.

Substituting these values into Equation 13 we obtain:

$$Q = 5.95 \times 10^{-16} \text{ Ci/mb/GeV protons/sec} \quad (14)$$

The total inelastic cross-section of oxygen is about 290 mb and thus the total activity produced in the ground water is

$$Q \simeq 1.7 \times 10^{-13} \text{ Ci/GeV/sec} \quad (15)$$

Comparing this with the estimate of 6.15×10^{-10} Ci/protons/sec at 30 GeV for the total activity produced, we see that < 1% of the total activity is produced directly in the ground water.

We may estimate the total activity in the earth of the shield, Q_E, by noting that

$$\frac{Q_E}{Q_W} = \left(\frac{1-f}{f}\right) \frac{\rho_E \sigma_E}{\rho_W \sigma_W} \frac{M_W}{M_E} \quad (16)$$

where the suffices E and W represent earth and water, respectively.

Assuming that the earth consists of chalk ($CaCo_3$) and 20% water (f = 0.2) the values to be substituted into Equation 16 are

$$f = 0.2; \quad \frac{\rho_E}{\rho_W} \simeq 2.0; \quad \frac{M_W}{M_E} \simeq \frac{1}{5.5}; \quad \frac{\rho_E}{\rho_W} = 5.6$$

Thus, typically, the total activity in the earth shield will be a factor of five to ten times higher than that produced in the water.

A comparison of the quantities of radioactivity produced using Equations 10, 15, and 16 is shown in the approximate ratio, $Q_{:total}:Q_{earth}:Q_{water}$ = 100:10:1. Roughly 90% of the total radioactivity is produced in the accelerator structure, 10% of the radioactivity in the surrounding earth shielding, and 1% in the ground water.

As we have mentioned in the introduction, large high-energy accelerators are buried underground to provide adequate radiation shielding. Substantial high-energy neutron fluxes will be generated in the earth shield, inducing radioactivity. The radioactive nuclides produced in the ground water might pass into the general ground-water system and therefore possibly into the public water supplies extracted from the area. In addition, the possibility that activity induced in the earth may be leached into the ground-water system must also be considered.

This assessment of a potential contamination of drinking water supplies falls into three stages:

1. Consideration of the possible radionuclides which could be produced in rock from a knowledge of the chemical composition of rock, in the dissolved substance in water, and directly in water itself.
2. Estimation of the yield of these radionuclides from the known production cross-section, radioactive half-life, particle flux densities, and energy spectra

Should the yield of radionuclides estimated at stage 2 be sufficiently high, then a third stage follows:

3. Estimation of the final specific concentration of radionuclides in local water supplies must be made taking into account site hydrology, dilution, radioactive decay, and chemical sorption

Several authors have reported the observation of radionuclide production in earth and water, either in laboratory simulations or directly in the accelerator shield. None of them is complete, but together they give a fairly comprehensive picture of the most important radionuclides of concern.

Radionuclide Production in Water

The most obvious potential source of radioactive contamination of ground-water systems arises from the production of radionuclides directly in the water. Thermal neutron capture in hydrogen and spallation reactions in oxygen and dissolved substances in water may result in a large number of radionuclides. Because these radionuclides are produced directly in water which is mobile, there might be a possibility of

their transfer from the site of activation (around the accelerator) and entry into local ground-water systems.

It is perhaps important at the outset to remark that up to the present time, no significant ground-water system contamination due to accelerator operation has been observed: However, it is certainly good health physics practice that such a possibility be investigated.

A review of studies of the production of radionuclides in water around accelerators prior to 1972 has been published by Stapleton and Thomas[5,50] and more recent work discussed by Patterson and Thomas.[51]

Initial interest in water activation around particle accelerators arose because of potential external radiation exposure hazards to personnel working close to cooling water systems. Thus, Rose et al.[52] identified short-lived oxygen spallation products in the dee cooling water of the Atomic Energy Research Establishment (AERE) 150-MeV synchrocyclotron. Distenfeld[53] has reported measurements of the inventory of ^{11}C, ^{22}Na, ^{7}Be, and ^{3}H in the Brookhaven AGS magnet cooling water. Similarly, measurements have been reported for ^{3}H in Nimrod cooling water at the Rutherford Laboratory.[54] Nelson[55] has reported one of the first studies of possible ground-water contamination due to a high-energy accelerator, in estimating radionuclide production near beam dumps of the SLAC 20-GeV electron linac. Middlekoop,[56] in a design study for a 300-GeV proton synchrotron, showed that spallation reactions in water could produce concentrations of ^{3}H and ^{7}Be many times greater than the maximum permissible concentrations recommended by the International Commission on Radiological Protection (ICRP).

Rindi[57] made detailed calculations of the radioisotopes produced in the cooling water of the CERN 300-GeV proton synchrotron and showed that the presence of large amounts of ^{7}Be can also cause external irradiation exposure from pipes and heat exchangers.

Table 3 lists the possible spallation products from ^{16}O with half-lives longer than 10 sec which will be produced directly in water (listed in order of increasing half-life).

Measurements of the production of radionuclides in water irradiated in accelerator environments have identified ^{11}C as the dominant short-lived radionuclide 1 to 5 hr after irradiation. ^{7}Be was the only γ-emitter with half-life greater than 10 hr produced in measurable quantities, and it was produced with a cross-section of about 10 mb in a variety of experimental conditions. The production of tritium under these conditions was consistent with a production cross-section of 30 to 35 mb.[5,54,58]

TABLE 3

Spallation Products from ^{16}O

Nuclide	Half-life
^{10}C	19 sec
^{14}O	71 sec
^{15}O	124 sec
^{13}N	10 min
^{11}C	20.5 min
^{7}Be	53 days
^{3}H	12.2 years

Gilbert et al.[4] have reported an extensive study of the distribution of particle flux densities in the earth shield of the CPS. Using this work, Stapleton and Thomas[5] have derived empirical expressions for the maximum specific activity, S_0, and the total activity, Q, produced at saturation in the water of the earth shield.

Assuming that the spallation products are proportional to beam power:

$$S_0 = 2.2 \times 10^{-20} \text{ Ci/l/mb/GeV/sec} \quad (17)$$

$$Q = 6.0 \times 10^{-16} \text{ Ci/mb/GeV/sec} \quad (18)$$

As an example, Stapleton and Thomas consider a 300-GeV accelerator with an intensity of 3.3×10^{13} proton per second of which 10% is lost due to inefficient beam extraction. In this case they estimate:

$$S_0 = 22\sigma \ \mu\text{Ci/l} \quad (19)$$

and

$$Q = 0.6\sigma \text{ Ci} \quad (20)$$

For ^{7}Be production, $\sigma = 10$ mb, and for ^{3}H production, $\sigma = 30$ mb (approximately). Thus, the maximum specific activities of ^{7}Be and ^{3}H produced in the ground water in the shield are 110 and 220 MPC, respectively.* Total quan-

* MPC for the general population.

tities of these nuclides in the shield are 6 and 18 Ci, respectively.

C. Radionuclides Resulting from Dissolved Solids in Water

Middlekoop[56] was the first investigator to estimate the specific activity due to irradiation of the impurities dissolved in ground water. His investigation was limited to those radionuclides produced by thermal neutron capture for water at a specific site. From a chemical analysis of the ground water of a chalk region in the United Kingdom (which was proposed for the construction of a 300-GeV proton accelerator[5]), Middlekoop identified 16 radioactive species that would be produced. Measurements of thermal neutron flux density in the earth shield of the CERN proton synchrotron[4] then facilitated estimates of the maximum specific activity which could appear in the ground water in the earth surrounding such an accelerator.[5] Table 4 summarizes these estimates. Inspection of the final column shows that no nuclides are produced in concentrations at saturation comparable to MPC[3], with the exception of ^{36}Cl. However, this radionuclide will be of no consequence because its half-life of 3×10^5 year will result in an extremely low production rate.

In the experiments of Stapleton and Thomas already referred to,[5,54,58] the presence of ^{32}P in the dissolved solids of irradiated ground water taken from the chalk site was detected. However, ^{32}P is fixed in chalk in the form of calcium phosphate and would not be expected to be mobile in ground water in chalk soil.[59]

Komochkov and Teterev[60] and Borak[61] reported γ-spectroscopy measurements performed in the cooling waters of the Dubna 700-MeV Synchrocyclotron and CERN 20-GeV proton synchrotron showing the presence of radioisotopes which were produced by corrosion of machine parts. ^{60}Co, ^{58}Co, ^{57}Co, ^{56}Co, ^{59}Fe, ^{56}Mn, ^{54}Mn, ^{52}Mn, and ^{22}Na were identified. However, these isotopes are absorbed in the ion exchange resins of the secondary cooling circuit, and the probability of finding them in water released to the environment is negligible, provided the backwash solutions from the filters are isolated from the environment.[66]

D. Radionuclides Produced in Earth

As in the case of ground water, several studies of the production of radionuclides in earth have been made and some of these results are summarized in Table 5.

From the chemical composition of the soil at the CERN site and measurements of particle flux densities in the CPS earth shield, Hoyer[62] calculated the specific activity of radionuclides to be expected in the soil. He concluded that only four radionuclides were produced in measurable quantities. To check his calculations, Hoyer compared his estimates with measured values of the specific activity of ^{45}Ca and ^{22}Na found in earth taken from several locations in the earth shield. Measured activities were, in general, lower by a factor of 3 than those calculated, which Hoyer attributed to leaching of these nuclides from the site by rain water. The production of tritium was not considered in this study.

In studying the radiological impact of the 500-GeV proton synchrotron at the FNAL, Borak et al.[63] irradiated glacial till and various clay soils in typical high-energy accelerator radiation fields. Table 5 summarizes the radionuclides identified in these soils, while Table 6 gives the measured macroscopic cross-sections for their production.

The average macroscopic cross-section determined for tritium in the ground water was 5.1×10^{-3} cm^2/g, assuming the water content of the soil was 14% by weight. This corresponds to a microscopic production cross-section of 152 mb which is a factor more than three higher than determined in water irradiations at the Rutherford Laboratory[54] and a factor of five higher than the more precise values of 30 to 35 mb tabulated by Bruninx.[64] It seems possible that this apparently high-tritium production cross-section is due to the production of tritium by spallation of constituent elements of the earth and direct transfer into the ground water.

Since operation of the FNAL 500-GeV accelerator, an extensive program monitoring the radioactivity in earth and ground waters at critical areas on the accelerator site has been developed.[13,65,66] Water samples are collected from wells and creeks and no accelerator-produced radionuclides have been detected in such samples. However, in some sumps which collect water from the footings around accelerator tunnels and enclosures and from drains under targets and beam dumps, tritium is routinely detected. Occasionally, low concentrations of

TABLE 4

Estimated Maximum Saturated Specific Activities from Thermal Neutron Absorption in Water Impurities Irradiated in the Shield of a 300 GeV Proton Synchrotron Situated on a Chalk Site[56]

Elemental impurity	Concentration in site water (ppm)	Production reaction of radionuclide	Half-life radionuclide	Activation cross-section (barn)	Isotopic abundance of target nuclei (%)	Saturated specific activity (μ Ci/ml) at flux of 10^7n cm^{-2} sec	ICRP Maximum permissible concentration for members of the general population (μc/ml)	Concentration in MPC corresponding to saturated specific activity
Boron	1.6	$^{10}B(n,p)^{10}Be$	2.5×10^6 years	<0.2	20	1.6×10^{-7}	10^{-4}[a]	2×10^{-3}
		$^{11}B(n,\gamma)^{12}B$	0.019 sec	0.050	80	1.4×10^{-7}	10^{-4}[a]	1×10^{-3}
Carbon	25.6	$^{13}C(n,\gamma^{14}C$	5.8×10^3 years	9×10^{-4}	1.11	4.8×10^{-10}	8×20^{-10}	6×10^{-7}
Fluorine	0.1	$^{19}F(n,\gamma)^{30}F$	10.7 sec	9×10^{-3}	100	1.2×10^{-9}	10^{-4}[a]	1×10^{-5}
Sodium	10	$^{23}Na(n,\gamma)^{24}Na$	15 hr	0.536	100	5.7×10^{-6}	2×10^{-4}	2×10^{-3}
Silicon	10.3	$^{30}Si(n,\gamma)^{31}Si$	2.62 hr	0.110	3.05	2.8×10^{-8}	9×10^{-4}	3×10^{-5}
Sulphur	7	$^{32}S(n,p)^{32}P$	14.3 days	0.0112	95.0	5.7×10^{-8}	2×10^{-5}	3×10^{-3}
		$^{33}S(n,p)^{33}P$	24.4 days	0.015	0.75	5.8×10^{-10}	10^{-4}[a]	6×10^{-6}
		$^{34}S(n,\gamma)^{35}S$	87.1 days	0.26	4.22	5.5×10^{-8}	6×10^{-5}	9×10^{-4}
		$^{36}S(n,\gamma)^{37}S$	5.04 min	0.14	0.014	9.2×10^{-11}	10^{-4}[a]	9×10^{-7}
Chlorine	15	$^{35}Cl(n,\gamma)^{36}Cl$	3.2×10^5 years	30	75.4	2.3×10^{-4}	8×10^{-5}	3×10^{0}
		$^{35}Cl(n,p)^{35}S$	87.1 days	0.19	75.4	1.5×10^{-6}	6×10^{-5}	3×10^{-2}
		$^{35}Cl(n,d)^{32}P$	14.3 days	$<5 \times 10^{-5}$	75.4	3.9×10^{-10}	2×10^{-5}	3×10^{-5}
		$^{37}Cl(n,\gamma)^{38}Cl$	37.5 min	0.56	24.6	1.3×10^{-6}	4×10^{-4}	3×10^{-3}
Calcium	79	$^{44}Ca(n,\gamma)^{45}Ca$	164 days	0.67	2.06	6.1×10^{-7}	9×10^{-6}	7×10^{-2}
		$^{46}Ca(n,\gamma)^{47}Ca$	4.9 days	0.25	3.3×10^{-3}	3.4×10^{-10}	5×10^{-5}	7×10^{-6}

[a] Values not listed, 10^{-4} μc/ml assumed.

TABLE 5

Radionuclides Identified in Earth or Water at Accelerator Laboratories

Laboratory	Accelerator	Soil type	Radionuclides identified: In soil	Radionuclides identified: In water	Ref.
CERN	28-GeV proton synchrotron	Molasse	^{7}Be, ^{45}Ca, ^{54}Mn, ^{22}Na	^{22}Na	62
Rutherford Laboratory	300-GeV proton synchrotron	Chalk	^{7}Be, ^{47}Ca, ^{43}K, ^{32}P, ^{47}Sc	^{7}Be, ^{11}C, ^{3}H	5
FNAL Batavia	500-GeV proton synchrotron	Glacial till, various clays	^{7}Be, ^{45}Ca, ^{60}Co, ^{51}Cr, ^{55}Fe, ^{59}Fe, ^{3}H, ^{22}Na, ^{46}Sc, ^{48}V	^{45}C, ^{3}H, ^{54}Mn, ^{22}Na	63
Stanford SLAC	1-GeV electron linear accelerator	Sandstone	^{7}Be, ^{58}Co, ^{59}Fe, ^{54}Mn, ^{22}Na, ^{46}Sc	^{54}Mn, ^{22}Na	67

TABLE 6

Macroscopic Cross-sections for Soil Normalized to Unit Flux Greater Than 30 MeV[63]

Sample soil depth	A-1 Glacial till		B-1 Gray sandy clay		B-2 Red sandy clay		B-3 Gray clay	
Nuclide	Activity (pCi/g)	$\Sigma\eta_i\sigma_{ij}$ (cm^2/g)	Activity (pCi/g)	$\Sigma\eta_i\sigma_{ij}$ (cm^2/g)	Activity (pCi/g)	$\Sigma\eta_i\sigma_{ij}$ (cm^2/g)	Activity (pCi/g)	$\Sigma\eta_i\sigma_{ij}$ (cm^2/g)
^{7}Be	7.9×10^{-3}	2.9×10^{-4}	9.9×10^{-3}	3.7×10^{-4}	8.7×10^{-3}	3.2×10^{-4}	7.2×10^{-3}	2.7×10^{-4}
^{51}Cr	4.7×10^{-4}	1.7×10^{-5}	1.0×10^{-3}	3.7×10^{-5}	7.6×10^{-4}	2.8×10^{-5}	8.3×10^{-4}	3.1×10^{-5}
^{22}Na	5.6×10^{-3}	2.1×10^{-4}	6.1×10^{-3}	2.3×10^{-4}	5.3×10^{-3}	2.0×10^{-4}	4.2×10^{-3}	1.6×10^{-4}
^{54}Mn	1.6×10^{-3}	5.9×10^{-5}	1.1×10^{-3}	4.1×10^{-5}	9.5×10^{-4}	3.5×10^{-5}	1.0×10^{-3}	3.7×10^{-5}
^{46}Sc	8.2×10^{-4}	3.0×10^{-5}	3.6×10^{-4}	1.3×10^{-5}	2.6×10^{-4}	9.6×10^{-6}	3.1×10^{-4}	1.1×10^{-5}
^{48}V	1.1×10^{-4}	4.1×10^{-6}	2.9×10^{-4}	1.1×10^{-5}	1.8×10^{-4}	6.7×10^{-6}	2.0×10^{-4}	7.4×10^{-6}
^{55}Fe	2.5×10^{-3}	9.3×10^{-5}	3.2×10^{-3}	1.2×10^{-4}	1.9×10^{-3}	7.0×10^{-5}	5.6×10^{-3}	2.1×10^{-4}
^{59}Fe	8.7×10^{-5}	3.2×10^{-6}	4.6×10^{-5}	1.7×10^{-6}	3.6×10^{-5}	1.3×10^{-6}	4.2×10^{-5}	1.6×10^{-6}
^{60}Co	8.9×10^{-4}	3.3×10^{-5}	3.9×10^{-4}	1.4×10^{-5}	3.0×10^{-4}	1.1×10^{-5}	3.6×10^{-4}	1.3×10^{-5}
^{45}Ca	4.4×10^{-3}	1.6×10^{-4}	5.4×10^{-4}	2.0×10^{-5}	8.1×10^{-4}	3.0×10^{-5}	4.3×10^{-4}	1.6×10^{-5}
^{3}H	2.3×10^{-2}	8.2×10^{-4}	2.9×10^{-2}	1.1×10^{-3}	9.0×10^{-3}	3.3×10^{-4}	1.4×10^{-2}	5.2×10^{-4}
^{3}H[a]	1.6×10^{-1}	5.9×10^{-3}	1.6×10^{-1}	5.9×10^{-3}	1.1×10^{-1}	4.1×10^{-3}	1.2×10^{-1}	4.4×10^{-3}

[a] Cross-sections per gram of water in the soil.

^{45}Ca and ^{22}Na are also reported. Baker reports that predictions of radionuclide concentrations in the soil outside the accelerators are now generally reliable. Measurements of particle flux density inside the accelerator tunnels and calculations of the hadronic cascade in the earth shielding by Monte Carlo techniques to predict activities in the earth usually result in good agreement with measured values in the soil.[65]

A similar study to that of Borak et al.[63] was carried out for the design of a 300-GeV proton synchrotron (which might be located in a chalk site, but was never constructed).[5] The radionuclides identified in chalk are shown in Table 5.

Finally, Thomas[67] has reported measurements of radionuclides produced in an earth beam dump by 1-GeV electrons from the Mark III electron linear accelerator of Stanford University. The significant production of radioactivity in the earth beam dump was dominated by photonuclear reactions with the constituent elements of the soil. Several studies of the development of electron cascades have been re-

ported in the literature with excellent bibliographies being given in the papers by Nelson et al.[68] and Bathow et al.[69-71] These studies show that the production of radioactivity is dominated by the electromagnetic cascade. More recent experiments in concrete[72] and earth[73] using 4-GeV electrons confirm these earlier findings.

Figure 10 shows the distribution of activity some 2 ft into the earth behind the end of the dump tunnel. The maximum specific activity was estimated to be ~4500 μCi/ft^3 (Figure 11), and the bulk of the activity was contained within a small volume (few cubic feet).

Figure 11 shows the vertical distribution of specific activity as a function of distance along the beam direction. A steady increase in the width of these distributions is suggested by the data (Figure 12), but the varying beam conditions and crude accuracy of the data do not permit detailed analysis.

The maximum specific activities observed in these vertical distributions are plotted as a function of position along the beam direction in Figure 13. A large build-up to the transition curve is not observed because the radioactivity present was produced over a prolonged period of time by beams of variable geometry. However, the longitudinal development of the electromagnetic cascade may be clearly seen. The slope of the activity distribution in its exponential region is 0.057/cm (or 0.033/gcm^{-2} assuming the density of earth to be 1.7 g cm^{-3}) and shows that the activity is produced by the products of the electromagnetic cascade whose development is controlled by the minimum value of the absorption coefficients of the elements constituting the earth.

The total quantity of γ-emitting radionuclides in the earth, with half-lives greater than a few days, was estimated to be 17 mCi. The beam dump had been in use for 3 years and the power dissipated was 2.8 MWhr during this period. After a decay time of 6 months, the total activity amounted to about 8 mCi and was almost all due to ^{54}Mn and ^{22}Na. The quantity of ^{22}Na produced at saturation corresponded to 150 mCi/kW. The data obtained from this measurement are interesting because the spatial distribution of radioactivity in the earth beam dump were measured.*

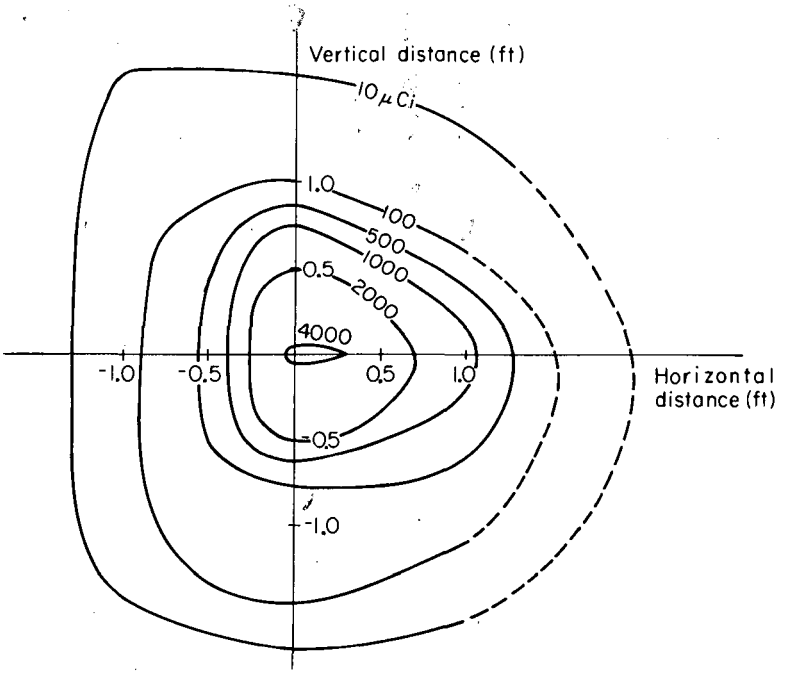

FIGURE 10. Contours of equal activity in the earth beam dump of a 1-GeV electron beam. The contours shown are at a depth of 2 ft.

* Since this review was completed, the authors have noted that the production of short-lived radionuclides in earth have been measured at the 70 GeV motor synchrotron laboratory at Serpukhov.[107] Sand and clay soils were irradiated and ^{11}C, ^{13}N, ^{24}Na, and ^{52}Mn were detected by γ spectrometry.

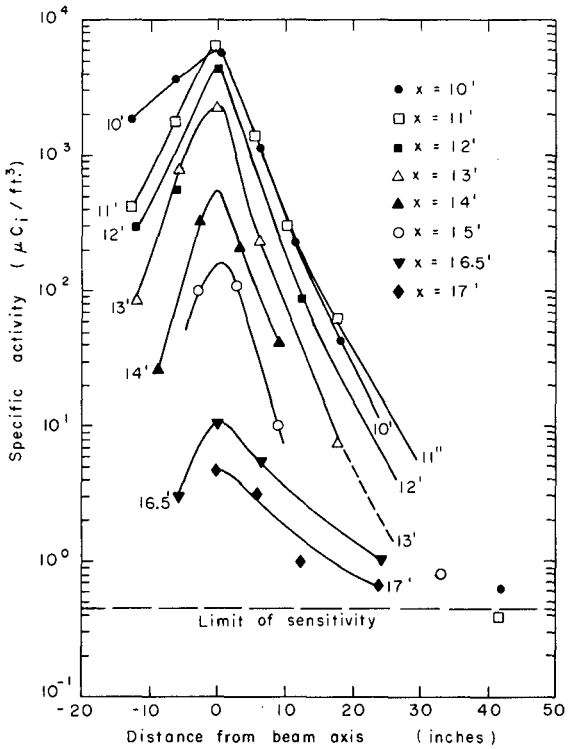

FIGURE 11. The vertical distribution of specific activity induced in earth by a 1-GeV electron beam for different distances of penetration into the dump.

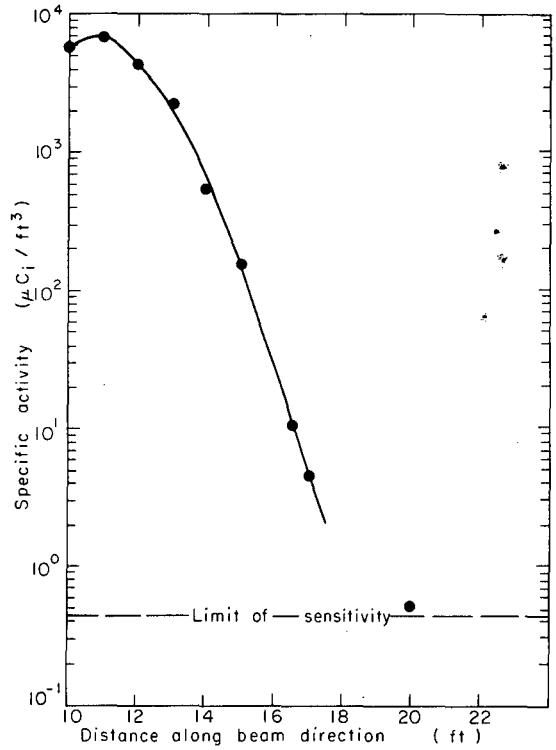

FIGURE 13. Maximum specific γ activity produced by a 1-GeV electron beam as a function of depth in earth.

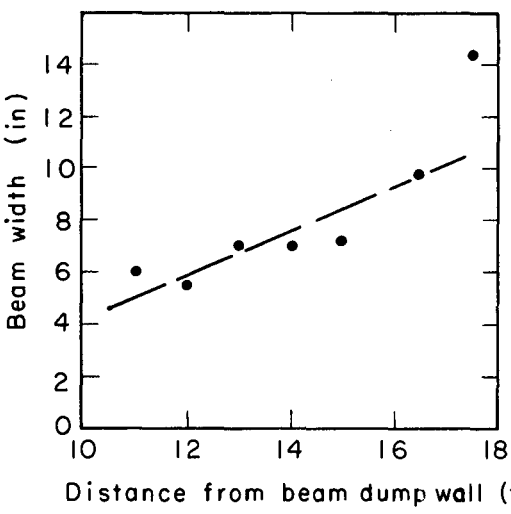

FIGURE 12. Increasing width (FWHM) of the distribution of γ activity as a function of depth in the earth produced by a 1-GeV electron beam.

E. The Migration of the Radionuclides through the Ground

The measurements described in Sections III.A to III.D show that a large number of radionuclides may be produced in the earth and ground water surrounding an accelerator.

As we said in Section III.B, the concentration of radionuclides in the ground water will then be controlled by the half-life of the radioactive species, solubility of the radionuclide, its possible dilution, and the site hydrology.

As we shall show, radionuclides with too short a half-life will decay so rapidly as to be of no potential hazard when they reach a public water supply. Conversely, if the half-life is too long, saturation activities will not be approached.

Knowledge of the hydrology of the accelerator site being studied will indicate the range of radioactive half-lives that are of interest. It is usually reasonable to study radionuclides with half-lives in the range: 10 hr < T < 100 year, but detailed investigation of site conditions will identify the appropriate range to be investigated. It should be noted that this general consideration limits the number of radionuclides that can appear in maximal quantities in ground-water systems. Therefore, in practice,

only a small number of radionuclides usually need to be studied in detail. In particular, the production of ^{3}H, ^{7}Be, ^{22}Na, ^{54}Mn, and ^{45}Ca merit study.

Not all the radioactivity produced will be in soluble chemical form. Thus, for example, less than 0.7% of the γ activity (principally ^{54}Mn and ^{22}Na) produced in the earth dump of the Mark III electron linac was soluble. Borak et al.[63] have made detailed studies of the solubility of the radionuclides produced in glacial till (Table 6). Of these radionuclides, only ^{45}Ca, ^{54}Mn, ^{22}Na, and ^{3}H were observed in leach waters. Of ^{45}Ca and ^{54}Mn, only a fraction of the activity (5 and 2%, respectively) was readily soluble.

We have seen that radioactive species may appear in the ground water surrounding an accelerator earth shield from the following sources:

1. Nuclear interactions or neutron capture directly in the water
2. Nuclear interactions or neutron capture in solids dissolved in the ground water
3. Transfer to the ground water of soluble radionuclides produced by nuclear interactions or neutron capture

However, the production of radionuclides in soluble form in the earth shield and the appearance of radioactive species in the ground water is not necessarily indicative of environmental harm — the radionuclides may be immobile. The greater part of radioactivity induced in the soil is confined to regions of high-radiation intensity and typically confined to a few locations and close to the accelerator. Stapleton and Thomas[5] state that 95% of the activity induced in earth is produced within 2 m of the outer wall of the accelerator tunnel of a proton synchrotron. In the absence of migration of any radionuclides from the activation zone, the radioactivity would increase to a final saturation determined by the accelerator intensity, the nuclear cascade process in the shield, and the macroscopic cross-sections for radionuclide production in rock and ground water.

However, it is possible that aquifers might be contaminated by activity washed out by water infiltrating the activation zone following rainfall. In this case, the maximum rate at which the radioactive nuclides can move is determined by the rate of movement of water in the aquifer. "A typical speed for water in deep aquifers is not more than 0.3 m/day, more than 1 m/day is quite exceptional and 0.03 m/day is not unusual."[74] As an example, Borak et al.[63] quote vertical-flow rates of 7 to 10 ft/year through the glacial till of the FNAL site.

Considerable studies have been made on the migration in the earth of the radionuclides derived from nuclear-fuel processing.

Radioactive materials do not, in general, move as rapidly as water. "They are held up by ion exchange with the rock or soil material by factors of 10^{-2} for Sr, 10^{-3} for Cs, 10^{-4} for Pu and Am, and 5×10^{-3} for Ra."[74] In a review on the movement of radioactive wastes buried in the ground, Mawson[75] reports that

> with few exceptions, absorption and exchange processes occur between the radionuclides and constituents of the soil . . . If the site is selected with care any radionuclides that enter the soil will progress quite slowly down the water table. Once in the ground water they will move faster, but still at a rate one to several orders of magnitude less than the rate of movement of the ground water. These statements apply to most cations — many anions move at about the same speed as the ground water.

The distribution coefficient, k, is a measure of the relative affinity of the radionuclide for earth compared with water. It is defined as the ratio of the concentration of ions absorbed by the soil to those remaining in solution at equilibrium. A large value of k indicates that ions preferentially adhere to soil and their migration is retarded.

The average velocity of ions through the earth, v_i, is related to the velocity of the water, v_w, by the equation:

$$\frac{V_i}{V_w} = \frac{1}{1 + k\,(\rho/p)} \tag{21}$$

where k = the distribution coefficient (milliliters per gram); ϱ = the bulk density of the rock; and p = the porosity of the rock (fraction of total volume of soil occupied by voids). For large distribution coefficients Equation 21 reduces to:

$$\frac{V_i}{V_w} = \frac{p}{k\rho} \tag{22}$$

As an example, the distribution in coefficient for ^{7}Be between water and chalk is ~4,500 and substituting the values: k = 4500, ϱ = 1.7 g cm^{-3}, and p = 0.50 into Equation 22, we see that beryllium ions move slowly than the ground water by a factor of about 15,000. Under these conditions migration rates would be so slow that radioactive decay will reduce the original activity to negligible levels.[76]

Experimental determination of the distribution coefficients would preferably be carried out under dynamic flow conditions by controlled column experiments which simulate field conditions. This is usually difficult in practice because the vertical-flow rate of water in highly compacted soils is usually very small. Columnar flow experiments with cored samples of undisturbed soil or rock are therefore usually prohibitively time consuming and channeling of water flow and wall effects of practical columns lead to inaccurate results.

In column experiments, to simulate water movement through a solid mass of chalk, persistent fissure formation made the use of a plug of consolidated finely powdered chalk infeasible. Recourse had to be made to columns of chalk prepared in granular form giving a system of high permeability.[76] Even with such columns, streaming occurred with a consequent overestimation of radionuclide migration. Column experiments are therefore extremely difficult, time consuming, and potentially inaccurate.

Static experiments for the determination of the distribution are much easier. Such experiments show that k is a function of the concentration of the radionuclides in water. Figure 14 shows the distribution of ^{7}Be between chalk and water and may be summarized by the equation:

$$k(c) = 1610\, C^{-0.12} \qquad (23)$$

where k(c) is the distribution coefficient for ^{7}Be between chalk and water measured in units of milliliters per gram and C is the concentration of ^{7}Be in water (in units of milligrams per milliliter). At an equilibrium concentration of 1 mg Be per gram of chalk, the distribution coefficient obtained from Figure 14 is 4500. The corresponding distribution coefficient obtained in column experiments is 4200.[76]

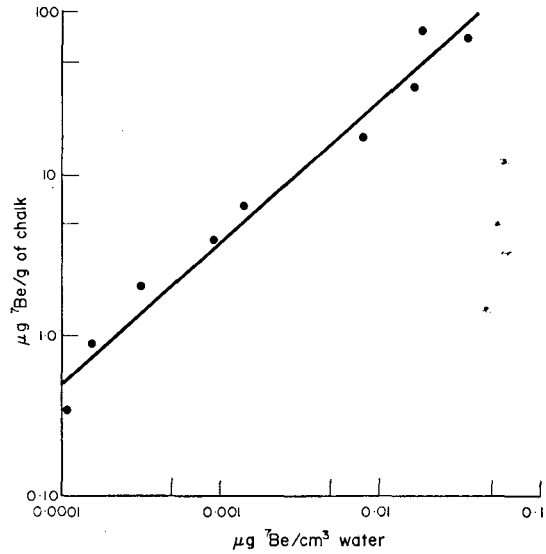

FIGURE 14. The sorption of beryllium in chalk.

Schroeder et al.[77] have also reported good agreement between distribution coefficients made under static and dynamic-flow conditions for glacial till provided the soil grain size is small and the concentration of radioactivity is low. Since this latter condition is met in the field conditions at high-energy accelerators, we may conclude that distribution coefficients determined by static experiments may be applied to dynamic conditions with reasonable accuracy.

Measurements of the distribution coefficients for ^{45}Ca and ^{54}Mn led Borak et al.[63] to conclude that these radionuclides would migrate very slowly through glacial till. ^{45}Ca "should decay before traveling any appreciable distance", and "^{54}Mn should not reach undesirable concentrations at distances far from the point of production." Hoyer reports a measured distribution coefficient of 10^3 for ^{45}Ca and estimates a value of 10^2 for ^{54}Mn between molasse* and water.[62].

Studies of the movement of ^{7}Be through chalk have also been reported.[76] The molecular species of ^{7}Be formed in water surrounding the accelerator tunnel will be in the form of a strongly hydrolyzed ion, similar to the radiocolloid described by Mellish et al.[78] In particular, ^{7}Be has been recognized as being a species which is very strongly absorbed onto surfaces from carrier-free solution; indeed, in solution

* Arenaceous rocks, typical of alpine orogeny, related to the Flysch formation.

in which the Be content is considerably less than the solubility product for the hydrolyzed cation, separations of carrier-free ^{7}Be may be made by a simple filtration.[79,80] Therefore, it would follow that this known sorption of tracer beryllium might result in holdup in the wet rock for periods sufficient to allow significant decay to occur and to reduce concentrations in ground water due to low leach rates from the regions of greatest yields from around the accelerator ring. We have already seen that the value of k of ~4500 was obtained between water and chalk.

Hoyer estimates k ~10^2 for ^{32}P at CERN.[62] This radionuclide was identified in irradiated chalk, but studies reported by Blythe[59] show that ^{32}P is predominantly fixed in chalk soils in the form of calcium phosphate and therefore would not be expected to be leached out in significant amounts by ground water.

In the case of ^{22}Na, there seems to be some significant difference between the observations of Hoyer, who determined a distribution coefficient of 10^2 at CERN, and those of Borak et al. at FNAL.[63] The latter workers found that, in the case of ^{22}Na, 10 to 20% of the activity is produced in a chemical form which is extremely soluble in water. In equilibrium, the distribution coefficient was determined to be 0.20 and the ion velocity about 40% of that of the ground water.

Of all the radionuclides produced in the earth and ground water, it is likely that only tritium will move freely in ground water without significant holdup due to absorption on rock surfaces. In static measurements of distribution coefficient, Borak et al. report that the quantity of tritium found in leach waters was consistent with the quantity produced in the free water in the soil. (They conclude that any tritium produced in spallation reactions in the constituent element of the earth is firmly bound, but this conclusion is not entirely consistent with the production cross-section for tritium to be expected — see Section III.D.) The distribution coefficient measured was very small, and thus the tritium will migrate with the same velocity as water through the aquifer.*

Therefore, it is probable that tritium may be the radionuclide that should be most carefully studied in ground water around accelerators, especially since increments above background should be readily detectable by straightforward measurements.

F. Potential Contamination of Drinking Water Supplies

From what has been stated, we can speculate that the possibility of significant contamination of drinking water supplies is extremely remote.

A detailed study of these phenomena would be extremely complex but Thomas has proposed a simple model that may be used to understand their magnitude.[50] This model is schematically shown in Figure 15 where an accelerator is buried underground. Radioactivity is induced in an "activation zone" close to the accelerator building. It is postulated that the radionuclides may be washed downward to the water table by rainfall. When they reach the water table they are transported to the boundaries of the accelerator laboratory. In the movement they are mixed with and diluted in the ground water. This water might be available for public use.

The specific activity, S, of the water available to the public is then given by:

$$S = D \sum_i \frac{\epsilon_i Q_i \left(1 - e^{-T_i/\tau_1}\right)_e - t_1/\tau_i}{M_i} \qquad (24)$$

where there are i radionuclides produced; D is a dilution factor; ϵ_i is the fraction of activity produced that migrates from the site of its production; Q_i is the total quantity of the the i^{th} radionuclide produced at saturation; T_i is the residence time in the activation zone; τ_i is the mean life of the i^{th} radionuclide; t_i is the transport time from leaving the activation zone to reaching the laboratory perimeter; M_i is the

* Recently, Balukova et al.[108] have measured the distribution coefficients of the radionuclides ^{7}Be, ^{22}Na, ^{32}P, ^{35}S, and ^{45}Ca in several different soils. For ^{7}Be, they determined distribution coefficients in the range 50 to 1600; for ^{22}Na, in the range 0.2 to 1.2; for ^{35}S, 0.4 to 2.3; and for ^{45}Ca, 4 to 14. Only two measurements were made for ^{32}P, and values of 16 and 18 obtained. The soils used were three types of loam (alluvial, limnetic and morainic) and two types of sand (coarse and fine). The authors conclude that the distribution coefficient is strongly dependent upon soil characteristics. However, in examples used by the authors, only ^{22}Na and tritium are potential contaminants of water supplies.

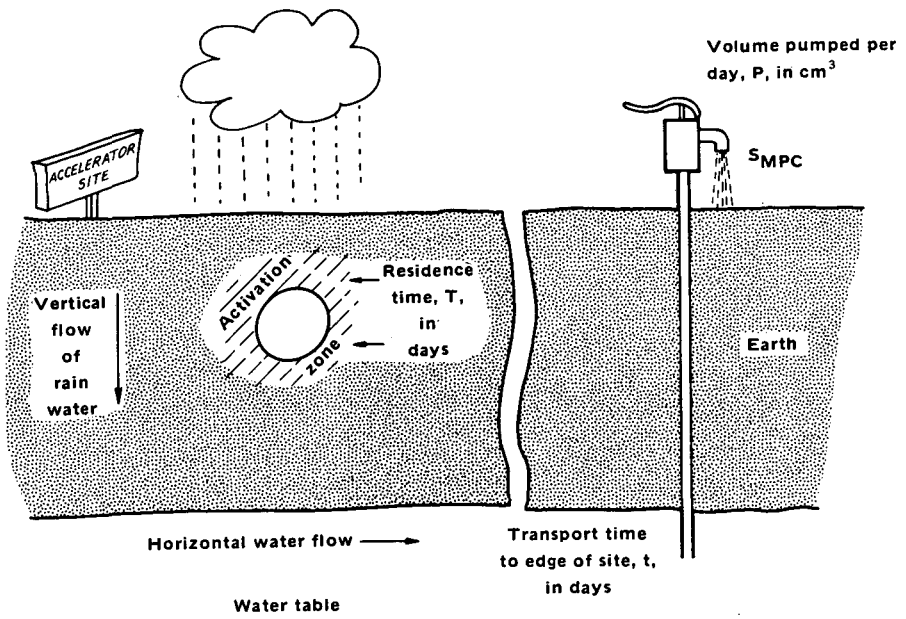

FIGURE 15. Model illustrating the mechanism by which accelerator-produced radioactivity may appear in ground water.

MPC of the i^{th} radionuclide; and S is measured in units of MPC. Equation 24 permits a crude assessment of the magnitude of the problem. The maximum rate of release of activity occurs at small residences times (T = 0) when all the activity-produced migrates (ε = 1) and the transport time to the site boundary are very short ($e^{-t_i/\tau_i} = 1$) when:

$$S_{MAX} = D \sum_i \frac{Q_i}{M_i \tau_i} \quad (25)$$

At an accelerator site where the water table is not disturbed by pumping, the outflow of water would equal the inflow from rainfall, and the radioactivity released would be diluted in a volume of water equivalent to the rainfall on the site.

If it is likely, as we have seen, that tritium is the only radionuclide of significance, the value of S_{MAX} reduces to:

$$S_{MAX} = D \frac{Q_H}{M_H \tau_H} \quad (26)$$

where the suffix H refers to tritium. Substituting the typical values:

$1/D = 10^{10}$ ml/day

$Q_H = 20$ Ci

$\tau_H = 17.6$ years

$M_H = 3 \times 10^{-3}$ μci/ ml (general population)

we obtain:

$$S_{MAX} = 1 \times 10^{-4} \text{ MPC} \quad (27)$$

Figure 16 gives examples of the concentration of several radionuclides calculated for a 500-GeV proton synchrotron, similar to the CERN 28-GeV proton synchrotron, losing 10^{12} protons per second to the shield.[50]

It was assumed that all the radionuclides produced in the earth and water in the shield were released directly to the ground water, transported to the site boundary in a short time (7 days), and diluted with a quantity of water equivalent to the net rainfall on the accelerator site (10^{10} ml/day). Inspection of Figure 16 shows that even under these extremely conservative assumptions, the specific activity of the water would never exceed 0.03 MPC and that this value is rather insensitive to residence time up to periods of 1000 days. It is, of course, a simple matter to generate similar curves for dif-

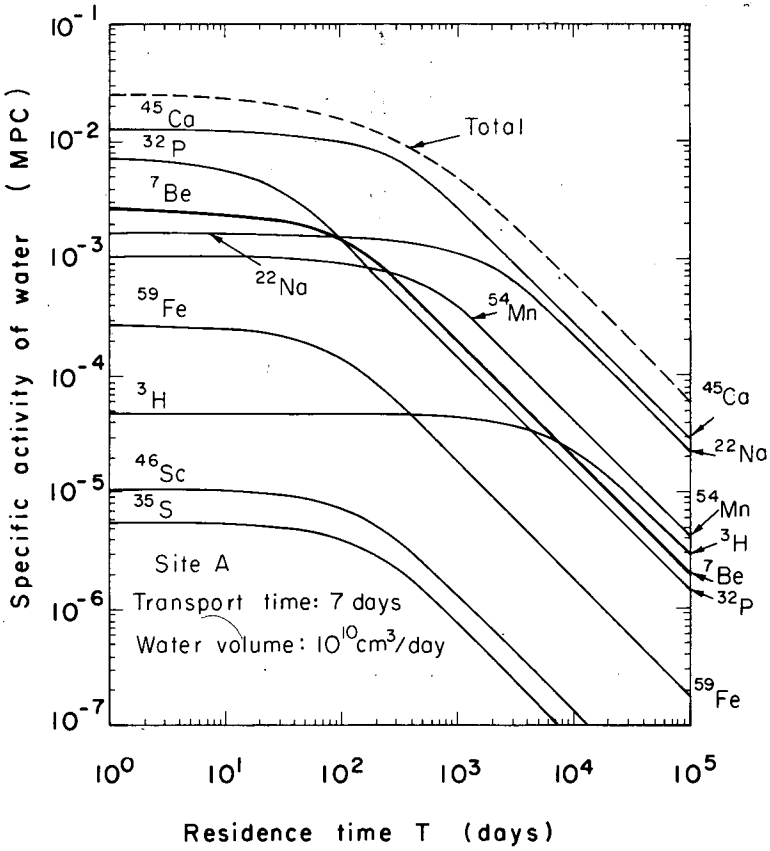

FIGURE 16. The specific activity of accelerator-produced radionuclides in the ground water at a hypothetical 500-GeV accelerator site, as a function of water residence time in the activation zone.[50]

ferent transport times to the site boundary. This crude treatment shows that the problem is not likely to be a serious one, but in actual practice, its magnitude is likely to be much smaller.

G. Population Dose Equivalent from Accelerator-produced Nuclides in Ground Water

The arguments presented in Section III.F. show that the concentration of the accelerator-produced nuclides will be insignificant at existing accelerator intensities.

The radioactivity from natural sources will in fact be higher by orders of magnitude than from accelerator-produced nuclides.

There have been no reported observations of accelerator-produced radionuclides in public water supplies and the consequent population dose equivalent is therefore effectively zero.

IV. RADIOACTIVITY PRODUCED IN THE ATMOSPHERE BY HIGH-ENERGY ACCELERATORS

A. Introduction

The second most important source of exposure of the general population to accelerator produced radiation is from radioactivity in the air.

However, typically, the magnitude of this exposure is many times smaller than that from "prompt" radiation. In fact, the magnitude of the exposure is often so small that no estimates of population dose equivalent have been made at some accelerator laboratories.

B. Radionuclides Produced in Air by Accelerator Operation

The main source of radioactivity in air is the

direct interaction of primary and secondary particles with constituent target nuclei of the air. A second source of airborne radioactivity is dust formed by natural erosion and wear or by maintenance on radioactive accelerator components. The third and final source is due to the emission of gaseous radioactivity from liquids irradiated in the accelerator-produced radiation environment.

1. Radionuclides Produced Directly in Air

During accelerator operation, radioactive nuclides are produced by the interaction of primary and secondary particles with the air in the accelerator halls. Spallation reactions in solid machine parts may also contribute to the formation of radioactive gases. If the air is confined in the accelerator hall, there will be no release of radioactivity outside during the operation of the machine. However, in such a case, a rather high concentration of radioactive gases may accumulate because the specific activity of several of the possible radioisotopes will reach saturation. Most of the present high-energy or high-intensity accelerators provide an air circulation and exchange with the outside, mainly for cooling reasons. The residence time of air inside the hall and consequently the irradiation time of the air is usually less than 30 min. This is so that the production of high concentrations of radioactive gases with a long half-life is minimal but the radioisotopes formed are continuously discharged in the atmosphere. Table 7 summarizes the target nuclei most abundant in air.

A summary of all the radionuclides with half-lives greater than 1 sec that may be produced from these target nuclei by thermal neutron capture (γ,n) and spallation reactions is given in Table 8.

With the exception of ^{3}H and ^{7}Be, the half-lives of possible products from irradiation of air are short, such that there will be some decay in the short time before they reach ground level from the chimney where they are discharged.

From the environmental point of view, the only significant radionuclides are ^{3}H, ^{7}Be, and perhaps ^{11}C, ^{13}N, and ^{15}O. However, the ^{3}H half-life is so long that its rate of production will be rather small.

Among the first reported measurements of radioactive gases generated by the interaction of accelerator produced particles with air components are those of Russel and Ryan[81] in 1965 who detected ^{15}O and ^{13}N in the air around a 70-MeV electron linac. The identification of the radionuclides was performed from the decay pattern and by γ spectroscopy; the radionuclides were produced by (γ,n) reactions with the ^{16}O and ^{14}N of the air from the γ-bremsstrahlung produced by the primary electrons. These authors calculated the occupational MPC for these radioactive gases for radiation workers and populations at large that were not available in the ICRP tables.[3,92] They also observed the production of ozone and of oxides of nitrogen by the ionization of the air. They studied the possible concentration of these radioisotopes in the environment by an atmospheric propagation model using the Sutton equation and concluded that the concentration levels were much lower than MPC. The same year, George et al.[82] reported similar findings at two 50-MeV electron linear accelerators; the identification was performed from the decay pattern of air samples measured with Geiger-Muller counters. These authors also performed calculations of the MPCs of the radioisotopes identified. Awschalom et al.[83] reported the possible identification of ^{14}O, ^{15}O, and ^{13}N in irradiated air, and N_2, CO_2, and O_2 at a 3-Gev Proton synchrotron.

In 1967, Rindi and Charalambus[84] reported a detailed calculation of all the possible radioisotopes which can be produced by interaction of the radiation produced from high-energy proton accelerators with air. They also reported finding ^{13}N, ^{11}C, ^{41}A, and possibly ^{85m}Kr in the

TABLE 7

Most Abundant Isotopes in the Atmosphere

Isotope	Percentage by volume in the atmosphere
^{14}N	78.1
^{16}O	21.2
^{40}A	0.46
^{15}N	0.28
^{18}O	0.04
^{12}C	0.015
^{17}O	0.008
^{36}A	0.0016

TABLE 8

Radionuclides with Half-life > 1 min which can be Produced in Air at Accelerators[90]

Radionuclide	Half-life	Emission	Parent element	Production reaction	Cross-section (mb)
$^{3}_{1}H$	12.2 years	β^-	C	Spallation	10
			N	Spallation	30
			O	Spallation	30
$^{7}_{4}Be$	53 days	γ, EC	C	Spallation	10
			N	Spallation	10
			O	Spallation	5
			A	Spallation	0.6
$^{11}_{6}C$	20.5 min	β^+	C	Spallation	30
			N	Spallation	10
			O	Spallation	5
			A	Spallation	0.7
$^{13}_{7}N$					
	10 min	β^+	N	Spallation	10
			N	(γ, n)	10
			O	Spallation	9
			A	Spallation	0.8
$^{14}_{8}O$					
	74 sec	β^+, γ	O	Spallation	1
			A	Spallation	0.06
$^{15}_{8}O$	2.1 min	β^+	O	Spallation	40
			O	(γ, n)	10
			A	Spallation	
$^{18}_{9}F$	1.85 hr	β^+, EC	A	Spallation	6
$^{24}_{10}Ne$	3.4 min	β^-, γ	A	Spallation	0.12
$^{22}_{11}Na$	2.6 years	β^+, γ	A	Spallation	10
$^{24}_{11}Na$	15 hr	β^-	A	Spallation	7
$^{27}_{12}Mg$	9.5 min	β^-, γ	A	Spallation	2.5
$^{28}_{12}Mg$	21.3 hr	β^-, γ	A	Spallation	0.4
$^{28}_{13}Al$	2.3 hr	β^-, γ	A	Spallation	13
$^{29}_{13}Al$	6.6 min	β^-, γ	A	Spallation	4
$^{31}_{14}Si$	2.6 hr	β^-, γ	A	Spallation	6
$^{30}_{15}P$	2.5 min	β^+, γ	A	Spallation	4.4
$^{32}_{15}P$	14.3 days	β^-	A	Spallation	25
$^{33}_{15}P$	25 days	β^-	A	Spallation	9
$^{35}_{16}S$	87 days	β^-	A	Spallation	23
$^{34m}_{17}Cl$	32.4 min	β^-, γ	A	Spallation	
$^{38}_{17}Cl$	37.3 min	β^-, γ	A	(γ, pn)	4
$^{39}_{17}Cl$	55 min	β^-, γ	A	(γ, p)	7
$^{41}_{18}A$	1.8 hr	β^-, γ	A	(n, γ)	610

air of the CERN 500-MeV proton synchrocyclotron and 28-GeV proton sychrotron by measuring the decay of the radioactive air in an airflow ionization chamber. They also calculated the occupational MPC for some gaseous radioisotopes not included in the ICRP tables.

Shaw and Thomas[85] reported finding ^{16}N, ^{15}O, ^{13}N, and ^{11}C in the air around an extracted beam from a 7-GeV proton synchrotron; the measurements were performed with a flow ionization chamber.

Awschalom et al.[86] studied the production of radioisotopes from Argon irradiated by primary and secondary particles produced by 3-GeV protons hitting a metallic target. By γ-spectroscopy of irradiated gas samples, they identified ^{41}A, ^{39m}Cl, ^{24}Na, ^{37}S, and possibly some other short-lived radioisotopes produced by A spallation.

In 1969, Höfert identified ^{15}O, ^{11}C, ^{13}N, and small amounts of ^{41}A in the air of the hall of the CERN 600-MeV synchrocyclotron with an air flow ionization chamber. He also calculated MPCs for these radionuclides for the submer-

sion case and concluded that the hazard due to induced radioactivity in air at CERN accelerators was negligible compared to radiation hazard from other sources.

Vialettes[88] identified, by γ spectroscopy, several radioisotopes in the air of a 560-MeV electron Linac: ^{13}N, ^{15}O, ^{11}C, ^{41}A, ^{38}Cl, ^{39}Cl, ^{7}Be, ^{24}Na, ^{57}Ni, ^{56}Mn, and ^{159}Gd. The author studied the possible nuclear reactions with air or machine components which produced these isotopes. He also calculated MPC for some of those radionuclides.

In 1972, Prantl and Baarli[89] reported finding small amounts of ^{7}Be in a creek at the CERN accelerators; however, due to the lack of systematic background measurements of ^{7}Be produced by cosmic rays, no final conclusions as to its origin could be drawn at that time. The same year, Rindi[90] made a detailed theoretical study of the production of radioisotopes in the air of a 300-GeV proton accelerator and of the disperison of these isotopes in the environment. He concluded that, under adverse atmospheric conditions coupled with particular machine use, concentrations of ^{7}Be and perhaps also of ^{3}H of the order of the MPC for the population at large could be detected at approximately 5 km from the air rejection shaft of the accelerator. In 1974, Peetermans and Baarli[91] reported some new calculations and measurements performed at the CERN 600-MeV proton synchrocyclotron estimating the concentration of radioactive gases in the surrounding region when the intensity of that accelerator was increased. ^{7}Be, ^{24}Na, ^{28}Mg, ^{31}Si, ^{32}P, and ^{33}P were identified in the ventilation air around an extracted beam by flow ionization chambers and γ spectroscopy on filters. The measured concentrations were in agreement with those calculated. New MPCs were calculated. These authors concluded that the annual contribution to the dose equivalent at the CERN boundaries due to radioactive isotopes in air would be about 5 mrem, a negligible fraction of that due to stray radiation, and that the eventual ^{7}Be surface pollution at distances up to 1 km from the boundaries would be barely detectable. Table 9 summarizes all the experimental data discussed in this section.

ICRP reports No. 2[3] and 6[92] do not contain MPCs for many of the radionuclides produced by accelerators. As we mentioned above, several authors have made calculations of the MPC for some of the radionuclides not discussed by the ICRP. Yamaguchi[93] has recently published a detailed calculation for many of the radionuclides of interest around accelerators. However, some differences of opinion are evident among the various authors concerning the dimension of the gas cloud to be considered in the calculation of the MPC for external irradiation and whether and when to use MPC for submersion or for internal absorption. These discrepancies are reflected in slightly different values for the MPCs as proposed by different authors. All the calculated values are summarized in Tables 10 and 11.

TABLE 9

Radionuclides Identified in the Air Around Several Accelerators

Laboratory	Accelerator	Radionuclides identified
RPI	50-MeV electron linac	^{15}O, ^{13}N
Saclay	330—560-MeV, electron linac	^{13}N, ^{15}O, ^{11}C, ^{41}A, ^{38}Cl, ^{7}Be
CERN	600-MeV proton synchrotron	^{11}C, ^{13}N, ^{41}A
PPA	3-GeV proton synchrotron	^{14}O, ^{15}O, ^{13}N, ^{11}C
RHEL	7-GeV proton synchrotron	^{16}N, ^{15}O, ^{13}N, ^{11}C
CERN	25-GeV proton synchrotron	^{13}N, ^{11}C, ^{41}A
BNL	30-GeV proton synchrotron	^{13}N, ^{11}C, ^{41}A,

2. Radionuclides Produced in Dust

Experience at several large accelerators tends to show that the potential exposure to radioactive dust for maintenance crews working in the accelerator vault is negligible.

Charalumbus and Rindi[94] have identified ^{54}Mn (~50%), ^{7}Be (~25%), ^{51}Cr (~7%), ^{59}Fe (~9%), and ^{48}V (~9%) as the radionuclides largely found in dust at the CERN 28-GeV proton synchrotron. Radionuclides produced by nuclear reactions in steel have also been identified as the largest components to radioactivity found in dust at the Saclay 500-MeV electron linear accelerator.[88] Even in the regions of highest radiation intensity at the CPS (external dose rates several rad/hr), Charalumbus and Rindi measured dust contamination levels of only 5 nCi cm^{-3} — well below MPC for the constituent radionuclides. These authors conclude that the

TABLE 10

MPC for Radiation workers as Calculated by Different Authors (μCi/cm^3 for 40 hr/week)

Radionuclide	Russel et al.[81] (submersion)	George et al.[82] (submersion)	Rindi and Charalambus[84] (submersion)	Hofert[a,87]	Vialettes[88]	Rindi[90]	Yamaguchi[93] (submersion)
^{15}O	2.3×10^{-6}	2×10^{-6}	3×10^{-6}	2.5×10^{-5}	1.8×10^{-6}	2×10^{-6}	1.9×10^{-6}
^{13}N	2.3×10^{-6}	2×10^{-6}	5×10^{-6}	3.4×10^{-5}	2×10^{-6}	2×10^{-6}	2.1×10^{-6}
^{3}H			2×10^{-3}				
^{7}Be			6×10^{-6}		1.2×10^{-6}	2×10^{-6}	
^{41}A			2×10^{-6}	4×10^{-5}	1.8×10^{-6}	2×10^{-6}	
^{11}C			8×10^{-6}	4.6×10^{-5}	2.1×10^{-6}	2×10^{-6}	2.5×10^{-6}
^{16}N			5×10^{-7}			5×10^{-7}	5.3×10^{-7}
^{38}Cl					2.1×10^{-6}	2×10^{-6}	
^{39}Cl					3.3×10^{-6}	3×10^{-6}	10^{-6}
^{56}Mn					6×10^{-7}		
^{57}Ni					4.6×10^{-7}		
^{159}Gd					3×10^{-7}		
^{6}He							1.6×10^{-6}
^{10}C							1.9×10^{-6}
^{15}C							5.3×10^{-7}
^{16}C							3.3×10^{-7}
^{17}N							2.4×10^{-7}
^{14}O							10^{-6}

[a] Thomas and Rindi report the values for a 10-m cloud and for radiations affecting the skin, as suggested by the author to be those to be applied to accelerator workers.

external radiation hazard is dominant inside the accelerator vault.

Busick and Warren[95] have concluded that chemical toxicity and external radiation exposure are the factors that limit the machining of radioactive accelerator components rather than the inhalation of radioactive dust.

The most direct method of determining if any potentially serious internal contamination problem exists is to determine the body burdens of accelerator-produced radionuclides in accelerator workers and to study possible contamination pathways.

Patterson et al.[96] have reported whole body counting and bioassay studies of 93 accelerator workers at the LBL. Of those workers studied, 79 (85%) bioassays indicated some β activity indicating environmental contamination. The body burdens measured ranged from 1 to 120 pCi.

A survey made in 1962 of ten members of the crew of a 60-in. cyclotron (no longer in operation) showed that seven persons had body burdens of ^{65}Zn ranging up to 9 nCi. Several previous studies of internal deposition of ^{65}Zn in accelerator workers at other laboratories had been reported.[97-100] The principal pathway for ^{65}Zn into the body is believed to be due to the inhalation of fumes during the soldering of radioactive copper.

Anderson and Schmidt[99] have reported the observation of ^{54}Mn, ^{22}Na, and ^{48}V in addition to ^{65}Zn in accelerator workers at the Lawrence Livermore Laboratory.

Despite the high incidence of some low-level internal β-contamination found by Patterson et al., they concluded that the lower internal burden found in personnel working with the newer accelerators in Berkeley indicated great improvement in operational procedures. The observation of zero or low body burdens in these people indicated adequate standards of cleanliness in working conditions and personal hygiene of accelerator personnel.

3. Gaseous Radionuclides Released from Water

In certain circumstances, radionuclides produced in liquids irradiated at accelerators may be released to the environment. For example, tritium produced by spallation reactions in magnet cooling water may be released by the evaporation of water spills and losses during magnet maintenance or replacement.

Warren et al.[101] have studied the production

TABLE 11

MPC for Population at Large as Calculated by Different Authors (μCi/cm³)

Radionuclide	Russel[81]	Rindi[90]	Peetermans and Baarli[91]	Yamaguchi[93] (submersion)
^{15}O	5×10^{-8}	2×10^{-8}	4×10^{-8}	4.3×10^{-7}
^{13}N	5×10^{-8}	2×10^{-8}	5×10^{-8}	4.7×10^{-7}
^{7}Be		2×10^{-8}	4×10^{-8}	
^{11}C		2×10^{-8}	6×10^{-8}	5.8×10^{-7}
^{14}O			1.5×10^{-8}	2.3×10^{-7}
^{16}N				1.2×10^{-7}
^{38}Cl		2×10^{-8}	7×10^{-8}	
^{39}Cl		3×10^{-8}	3×10^{-8}	2.4×10^{-7}
^{41}A		2×10^{-8}	4×10^{-8}	
^{3}H			2×10^{-7}	
^{10}C			2.5×10^{-8}	4.3×10^{-7}
^{18}F			9×10^{-8}	
^{24}Ne			1.3×10^{-8}	
^{22}Na			3×10^{-10}	
^{24}Na			5×10^{-9}	
^{27}Mg			4×10^{-10}	
^{28}Mg			2×10^{-8}	
^{18}Al			4×10^{-8}	
^{29}Al			4×10^{-8}	
^{31}Si			3×10^{-8}	
^{30}P			4×10^{-8}	
^{32}P			2×10^{-9}	
^{33}P			6×10^{-9}	
^{35}S			9×10^{-9}	
^{37}S			4×10^{-8}	
^{38}S			4×10^{-8}	
^{6}He				3.6×10^{-7}
^{15}C				1.2×10^{-7}
^{16}C				7.4×10^{-8}
^{17}N				5.5×10^{-8}

of CO_2 which acts as a carrier for ^{11}C and ^{15}O produced in water beam dumps at the Stanford Linear Accelerator Center.

C. Magnitude of Radionuclide Production in Air

1. Fundamental Approach

The total specific activity, S, of an enclosed volume of radioactive air near an accelerator may be written as:

$$S = C \sum_{ijk} N_j \int_{E_{ijk}}^{E_{k_{MAX}}} \sigma_{ijk}(E)\, \phi_k(E)\, dE \; (1 - e^{-\lambda_i T})\, e^{-\lambda_i t} \qquad (28)$$

where S is the total specific activity of radioactive air (per liter); C is a constant; i represents the radionuclide of type i; j represents the target nuclide, j; k represents the interacting particle, γ, p, n, etc.; N_j is the number of target nuclei of type j in a liter of atmospheric air; $\sigma_{ijk}(E)$ is the cross-section for the production of the radionuclide of type i from the target j by a particle k at energy E; $\phi_k(E)$ is the flux density of particles of type k between E and E + dE; E_{ijk} is the threshold for the reaction i → j by a particle of type k; $E_{k_{max}}$ is the maximum energy of particles of type k; λ_i is the decay constant of the radionuclide i; T is the irradiation time; and t is the decay time.

Equation 28 may be simplified considerably by two approximations.

1. Production by only three modes is considered:
   a. Thermal neutron capture
   b. High-energy particle spallation
   c. γ,n reactions [k = γ, th, HE]

2. The integrals of Equation 28 are replaced by average fluxes and cross-sections:

$$\int_{E_{ijk}}^{E_{k_{max}}} \sigma_{ijk}(E)\,\phi_k(E)\,dE = \langle \sigma_{ijk} \rangle \Phi_k \quad (29)$$

Thus Equation 28 simplifies to:

$$S = C \sum_i \left[\sum_j \Phi_\gamma N_j \bar{\sigma}_{ij_\gamma} + \sum_j \Phi_{th} N_j \bar{\sigma}_{ij_{th}} + \sum_j \Phi_{HE} N_j \bar{\sigma}_{ij_{HE}} \times (1 - e^{-\lambda_i T})\, e^{-\lambda_i t} \right] \quad (30)$$

where Φ_γ, Φ_{th}, and Φ_{HE} are the average photon, thermal neutron, and high-energy particle flux densities, and $\sigma_{ij\gamma}$, σ_{ijth}, and σ_{ijHE} are the corresponding average cross-sections. To use the simple expressions, one must determine which nuclides are of greatest concern. Radionuclides with half-lives less than 1 min are of no concern, decaying to negligible activities before personnel may enter the accelerator room. They may also be similarly discounted with respect to exposure from gases leaking from the accelerator room during operation. Long-lived activities, on the other hand, may be discounted because of their low production rate. Therefore, it is not possible to produce ^{7}Be or ^{3}H at levels higher than a small fraction of saturated specific activity. Because of the extremely small thermal neutron absorption cross-section of ^{18}O and its low isotopic abundance, no significant quantity of ^{19}O would be expected. Such arguments suggest that only four radionuclides need be considered — ^{15}O, ^{13}N, ^{11}C, and ^{41}A.

Equation 30 assumes that the irradiated volume of air is static. However, generally, the air is changed in accelerator rooms two or three times per hour. (There are exceptions to this rule. For example, at the Stanford Linear Accelerator, air is not continuously released from the accelerator housing.[102] Exhaust fans are turned on after a delay period following the end of accelerator operation. Therefore, short-lived radionuclides are confined to the accelerator housing.) Even in cases where the accelerator room is not ventilated, normal leakage may amount to ~ 10% of the volume of enclosed air per hour. Unless special steps are taken to prevent air from leaving the accelerator room, its residence time is then always considerably less than 1 day.

The influence of air changes on the specific activity of air may be taken into account by substituting an effective decay constant λ_i' in place of λ_i in Equation 30, where λ_i' is given by:

$$\lambda_i' = \lambda_i + \frac{D}{V} \quad (31)$$

where D is the ventilation rate and V is the volume of the accelerator room.

Equation 30 has been used by several authors to calculate the concentration of radionuclides at different accelerators and has proved to yield rather precise results. Table 12 shows a comparison between measured and calculated concentration for the CERN 600-MeV proton synchrocyclotron as reported by Peetermans and Baarli.[91] Figure 17 shows a comparison of measured and calculated decay curves as reported by Rindi and Charalambus.[84]

2. Empirical Approach

An alternative approach to that outlined in Section IV.C.1 which requires some knowledge of average particle flux densities in the accelerator room is to proceed by assuming:

1. A fraction, P, of the primary beam generates secondary particles with multiplicity B(E).
2. The interactions of these secondary particles produce radionuclides in the air.

The total production rate of radionuclides, N, in air is then:

$N = p\ I\ B(E)$ in nuclei per gram. (the total activity produced at saturation is then: $\frac{N}{3.7 \times 10^{10}}$ Ci) (32)

TABLE 12

Measured and Calculated Specific Activity in Air of some Long-lived Isotopes Leaving the CERN 600-MeV Synchro-cyclotron ISOLDE Area[91] (pCi/cm³)

Isotope	Half-life	Measured	Calculated
^{3}H	12.26 years	—	1.6×10^{-5}
^{7}Be	53.6 days	2.7×10^{-4}	3.2×10^{-4}
^{24}Na	15 days	3.6×10^{-5}	4.8×10^{-5}
^{32}P	14.5 days	6.0×10^{-6}	8.4×10^{-6}
^{33}P	25 days	2.0×10^{-6}	4.5×10^{-6}
^{41}A	1.83 hr	—	2.5×10^{-2}

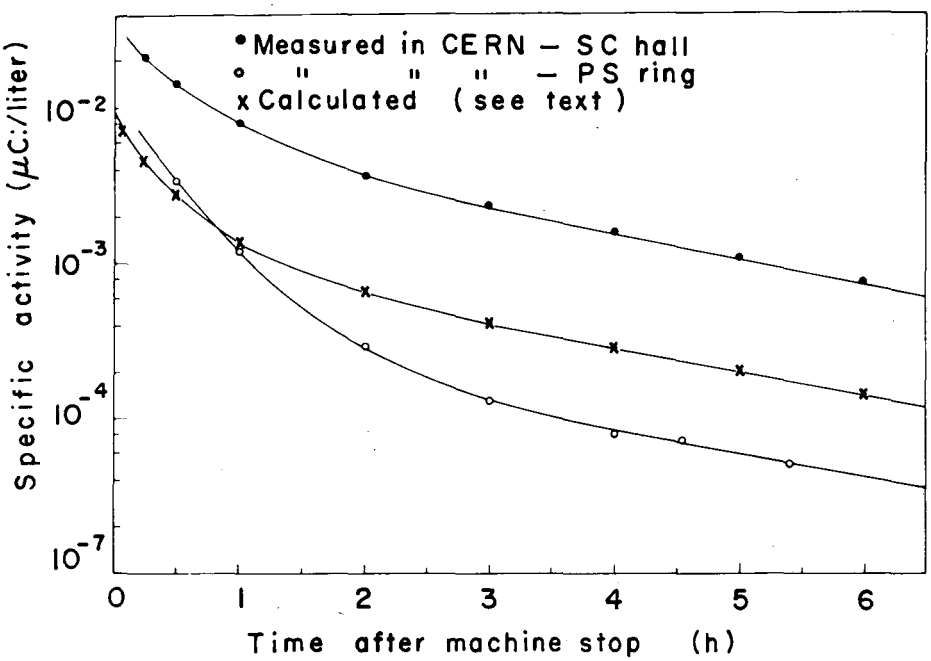

FIGURE 17. Typical decay curves of radioactive air as measured at the two CERN accelerators and computed decay calculated assuming that the contribution of radioisotopes is as follows: ^{41}A (14%), ^{11}C (31%), ^{13}N (47%), ^{15}O (8%).[84]

(the total activity produced at saturation is then: 3.7×10^{10}Ci)

The specific activity of radionuclide i from the target nucleus j is then:

$$A_{ij} = \lambda_{ij} \frac{\sigma_{ij}}{\sigma_j} F_j N \qquad (33)$$

where $\sigma_i = \Sigma \sigma_{ij}$ is the sum of the production cross-section for all possible radionuclides from the target nucleus j. F_j is the fraction by weight of the target element, j, in air.

The variation of multiplicity with energy has been studied by several authors and is usually expressed in the form:

$$B(E) \propto E^{n} \qquad (34)$$

At present, there is no general agreement as to the value of the parameter n. The value $n = 1$, which predicts that the total activity produced is proportional to the accelerator beam power, is only true under those conditions where the hadronic or electromagnetic cascades are well developed. However, it does represent a conservative limit and seem to work well for electron

TABLE 13

Maximum Values of Specific Radioactivity of the Air Measured at the CERN Accelerators (5 min after machine stop)[84]

Location	Total (μCi/l)	Contribution from different radioisotopes
In the ring of the CERN proton synchroton (near target region)	$\simeq 10^{-2}$	$^{13}N \simeq 50\%$; $^{11}C \simeq 30\%$; $^{41}A < 10\%$; other isotopes > 10%
In the hall of the CERN synchrocyclotron (near target region)	$\simeq 3.5 \times 10^{-2}$	$^{11}C \simeq 55\%$; $^{41}A \simeq 22\%$; $^{13}N \simeq 12\%$; other isotopes $\simeq$ 10%
In the extracted 600-MeV proton beam of the CERN synchrocyclotron	8	$^{11}C \simeq 67\%$; isotopes with halflife < 20 min $\simeq$ 32% (^{85m}Kr present; no ^{41}A)
Near a target placed in the path of the extracted 600-MeV proton beam of the CERN Synchrocyclotron	2×10^{-1}	$^{11}C \simeq 23\%$; isotopes with halflife < 20 min $\simeq$ 76% (^{85m}Kr present; no ^{41}A)

TABLE 14

Calculation of the Quantity of Radionuclides Released from the Stack of the ISOLDE Facility at the CERN 600-MeV Proton Synchrocylotron[91]

Half-life	Radionuclides	Curies released/a
1 min	^{10}C	1.3×10^2
1 min $\leq \tau_{1/2} \leq$ 1 hr	^{11}C,[a] ^{13}N,[a] ^{14}O,[a] ^{15}O,[a] ^{24}Ne, ^{27}Mg, ^{28}Al, ^{29}Al, ^{30}P, ^{37}S, ^{34m}Cl, ^{38}Cl, ^{39}Cl	1736
1 hr $\leq \tau_{1/2} \leq$ 1 day	^{18}F, ^{24}Na, ^{28}Mg, ^{31}Li, ^{38}S, ^{41}A	2.5
1 day $\leq \tau_{1/1} \leq$ 1 month	^{32}P, ^{33}P	7.3×10^{-3}
1 month < $\tau_{1/2} \leq$ 1 year	^{7}Be,[a] ^{35}S	1.9×10^{-2}
1 year < $\tau_{1/2}$	^{22}Na, ^{3}H[a]	9.1×10^{-3}
Total		1869 Ci/a

[a] Indicates dominant radionuclide(s).

accelerators. For proton accelerators, where the primary hadron cascade may not have reached equilibrium in the accelerator structure, values of n of 0.25,[103] 0.3,[104] 0.7,[103] and 1.0[4] have been suggested by different authors.

D. Impact on the Environment

The calculation of population exposure resulting from the release of gaseous radionuclides is normally performed according to the following steps:

1. Measurement or calculation of the concentration of the different radioisotopes released at the ventilation stacks of the accelerators
2. Calculation of the transport of the gases outside the boundaries of the laboratory; this is generally done by applying the Sutton equation for some average meteorological conditions
3. Conversion of the radioactive gases concentrations to dose equivalent to an exposed individual by using the MPC values
4. Summation of the total number of exposed individuals and their dose equivalent to give the total population dose

Some examples of concentrations of radionuclides in air produced inside accelerator halls or released from stacks are reported in Tables 13 and 14, respectively. Table 13 shows measured values while Table 14 reports values calculated assuming a 3×10^{13} protons per second proton beam incident upon a 30-g thorium target, with a proton beam path in air of 2 m.

Inspection of these tables shows that four radionuclides dominate the short-lived group (τ < 1 hr) — ^{10}C, ^{11}C, ^{13}N and ^{15} — which accouns for 99.8% of the total activity released. Of the longer lived radionuclides only ^{41}A,^{7}Be, and ^{3}H are released in significant quantities.

Steps 2, 3 and 4 above can be summarized in a general equation. Thomas[17] has described the use of the following expression to calculate the population dose equivalent resulting from the release of a given radionuclide that applies for the LBL but can be easily generalized.

$$M = \sum_{i=1}^{n} \left[\sqrt{\frac{2}{\pi}} \left(\frac{n}{2\pi} \right) \frac{f_i Q R}{u} \int_{r_0}^{\infty} \frac{N_i(r)}{\gamma \sigma_z(r)} dr \right] \quad (35)$$

where n is the number of sectors in which the region surrounding the rejection points has been divided (this division is decided by the wind direction frequencies); f_i is the fraction of time in which the wind blows toward a given sector; Q is the total quantity of radionculide released (in curies); R is the dose equivalent conversion factor for the given radionuclide (man rem per curie second per cubic meter);[106] u is the average wind velocity (in meters per second); r is the distance from the rejection point; $N_i(r)dr$ is the total number of people in the i^{th} sector in the region between r and r + dr; r_0 is the distance of closest approach to the laboratory; and $\sigma_z(r)$ is the vertical dispersion coefficient (in meters).

The integral can be simplified into a summation by subdividing each sector into m regions in which the population density may be assumed to be constant.

The number of residents at a distance r from the rejection point in the j^{th} region of the i^{th} sector is then given by:

$$_jN_i(r) = \frac{2\pi r}{n} \sigma_{ij} dr \quad (36)$$

where σ_{ij} is the population density.

The expression between brackets in Equation 35 can be expressed by:

$$_jM_i = \sqrt{\frac{2}{\pi}} \frac{f_i Q R \sigma_{ij}}{\bar{u}} \int_{r_{j-1}}^{r_j} \frac{dr}{\sigma_z(r)} \quad (37)$$

and the population dose equivalent is then expressed by:

$$M = \sum_{i=1}^{n} \sum_{j=1}^{m} {}_jM_i \quad (38)$$

From the meteorological statistics for the region under study, $\sigma_z(r)$ can be given an analytical expression as a function of r such that the integral in Equation 37 can be evaluated.

It is customary at accelerator centers to report yearly on environmental monitoring results. Several centers perform continuous measurements of gaseous radioactivity in air, in addition to radioactivity deposited on filters, and also periodically investigate the radioactivity on ground, water, and plants around the boundaries of the center.

At the Fermi Laboratory in Batavia, where a 300-GeV proton synchrotron is located, the annual offsite exposure from airborne release was estimated to be about 9.1 man rem, 1/10 of the exposure from external radiation during 1975.[66]

At the LBL where several proton and heavy ion accelerators are located, the estimated population dose from radionuclide release was 0.3 man rem, mainly due to ^3H and ^{14}C, and equivalent to 8% of the dose equivalent from prompt radiation. However, these radionuclides were released from chemistry laboratories and not due to accelerator operation.[105] In addition to the air measurements at the monitoring stations, a search for possible contamination from ^7Be was made by measuring the radioactivity of bracken ferns collected around the center and at different locations several miles away. Table 15 shows the results of these measurements. Given the different rainfall and absorption conditions at the various locations, large variations in the ^7Be content in the fern are expected; improper sampling methods can lead to errors up to one order of magnitude. In order to properly interpret such data, it is therefore important to fully understand the total deposition mechanisms. Table 15 shows data of the ^7Be concentration on bracken fern collected under carefully controlled conditions from various sites in northern California. The ^7Be concentrations are shown to be independent of location, within the accuracy of the measurement (estimated to be about 30%). With further study, the samples of bracken fern may be developed as a convenient and reliable monitor of accelerator-produced ^7Be.

At CERN in Geneva, where a 600-MeV synchrocyclotron and a 28-GeV proton synchro-

TABLE 15

Measurements of ^{7}Be in Samples of Bracken at LBL[17]

Location	Collection date	Specific activity of ^{7}Be counts per minute per centimeter of fern
Smith River U.S. Route 199 ~15 miles east of Crescent City 370 miles north of Berkeley	5/5/73	1.80
Overpack Grove U.S. Route 101 Near Richardson's Grove ~200 miles north of Berkeley	5/5/73	1.76
Marin County, near Nicascio ~30 miles northwest of Berkeley	5/17/73	1.74
University of California, Berkeley Seismograph Tunnel ~½ mile south of LBL site on upper west-facing slope of Berkeley Hills	2/15/73	2.12
Caldecott Tunnel State Route 24 ~2 miles southeast of LBL east side of Berkeley Hills	2/23/73	1.40
	4/4/73	1.39
	5/8/73	0.95[a]
Santa Cruz Mountains ~70 miles southwest of LBL	1/26/73	1.71
Fish Ranch Road ~2 miles southeast of LBL eastside of Berkeley Hills	2/23/73	2.06

[a] 1.42 counts per minute per gram when corrected for decay.

tron are located, the gross β activity of air samples show a seasonal trend similar to that found at other European monitoring stations (Figure 18). This similarity in trends is also reflected in the β activity of rain water measured at CERN and Le Vesinet, near Paris (650 km from CERN), (Figure 19B). However, differences in the γ-activity of rainwater are evident between Le Vesinet and Paris. The ^{7}Be content of rainfall at CERN shows much larger fluctuations than at Le Vesinet (Figure 19A). γ-Spectrometry of air-sampler filters shows that, while the activity of γ-emitting nuclides from nuclear weapons fallout show similar trends at both laboratories, fluctuations in ^{7}Be activity in air at CERN are much larger than those found at Le Vesinet (Figure 20). These data tentatively tend to suggest that accelerator operation at CERN produces detectable quantities of ^{7}Be close to the high-energy accelerators, corresponding to periods of high-intensity operation. Of course, they would be more convincing if the control data were obtained at a site closer to CERN than Le Vesinet (which is ~ 400 km distant). However, the radioactivity of rainfall samples in this region of western Europe is believed to vary little with location, at the same altitude.

V. CONCLUSIONS

The radiological environmental impact of high-energy accelerators is qualitatively different from most other nuclear facilities. Prompt radiation — produced when the accelerator is in operation — is the principal source of population exposure. For high-energy, high-intensity facilities, neutrons generally are the principal component of this prompt radiation field. At some electron facilities, or thinly shielded proton accelerators, photons may be a significant source of dose equivalent, while at the highest energies, muons have been detected. The magnitude of population dose equivalent due to high-energy accelerator operation is estimated to be in the range 50 to 1000 man rem/rem at

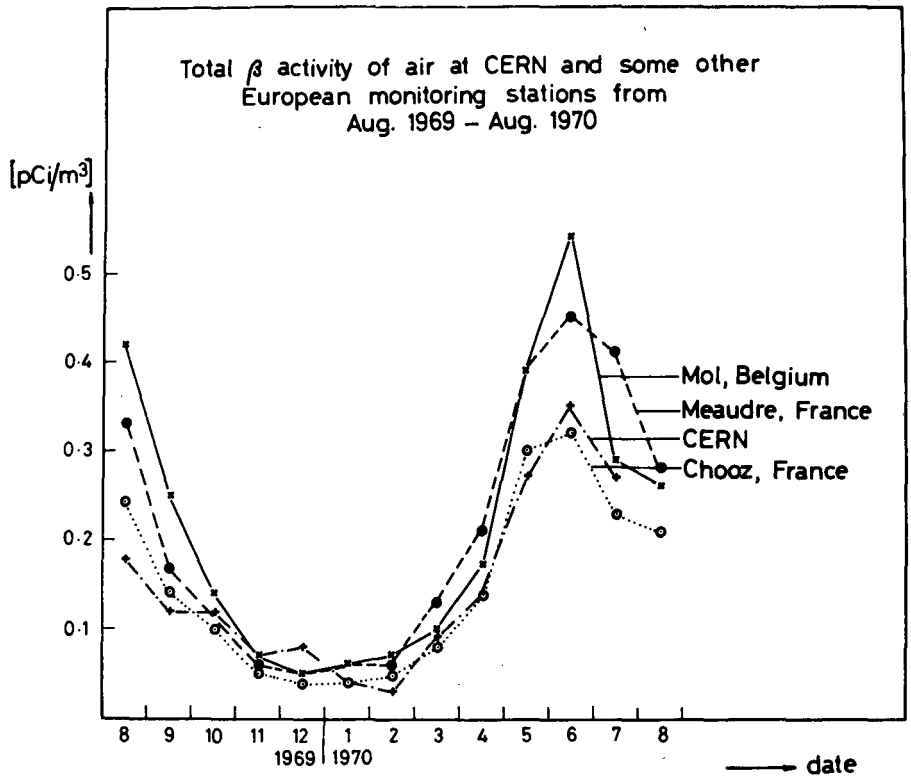

FIGURE 18. Seasonal variation of gross β activity in air samples at several European centers.

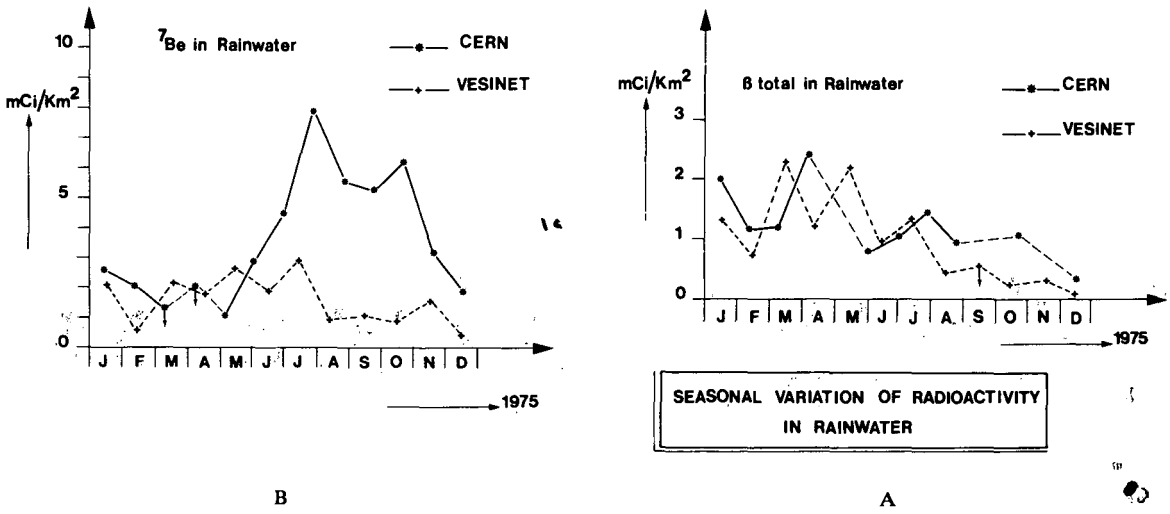

FIGURE 19. Monthly variation of radioactivity in rainwater at (A) CERN and at (B) Le Vesinet (Paris).[23]

the site boundary. Typical annual dose equivalents at accelerator boundaries are ~10 to 50 millirem, with resultant population dose equivalents of the order of ~10 man rem.

The production and release of radionuclides to the atmosphere is the other potential source of population exposure. Relatively long-lived radionuclides such as ^{41}A, ^{7}Be, and ^{3}H are of potential concern, but the population dose equivalent from the source is at least an order

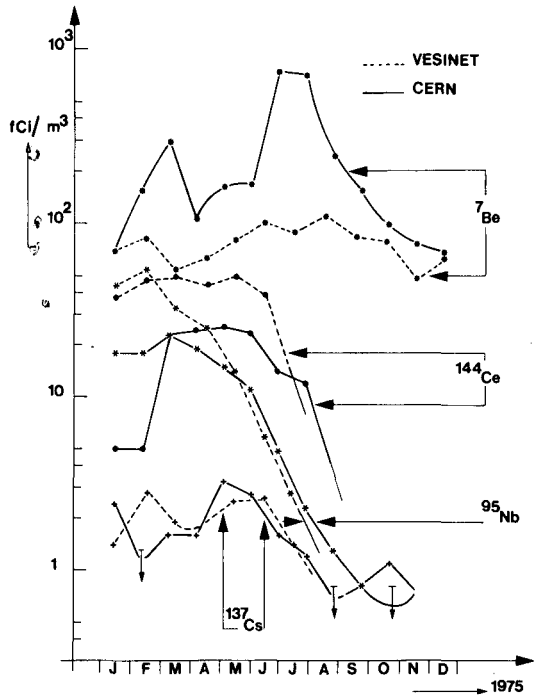

FIGURE 20. Monthly variation of identified airborne radionuclides at CERN and at Le Vesinet (Paris).[23]

of magnitude lower than that due to prompt radiation. Observations of the concentration of ^{7}Be in air, rainwater, on the ground surface, possibly supplemented by deposition measurements on vegetation, provide means of monitoring possible environmental contamination.

A significant concentration of accelerator-produced radionuclides has not yet been reported in ground-water systems near high-energy accelerators — but calculation shows that none is to be expected. Tritium is the only likely radionuclide to move freely in the ground water. No significant population exposure from this source is expected at present energies and intensities.

Acknowledgments

We are grateful to many colleagues for invaluable discussions during the preparation of this article. In particular, J. Baarli and J. W. N. Tuyn of CERN, A. Hull of Brookhaven National Laboratory, S. Baker of Fermi National Accelerator Laboratory, T. Borak and J. Sedlet of Argonne National Laboratory, G. B. Stapleton of the Rutherford High Energy Laboratory, D. Busick and W. P. Swanson of the Stanford Linear Accelerator Center, and H. P. Cantelow, A. R. Smith, and L. D. Stephens of the University of California Lawrence Berkeley Laboratory have freely made their data and suggestions available. P. Pellerin, Director, Service Central de Protection contre les Rayonnements Ionisants, Le Vesinet, permitted us to quote data on the radioactivity of air and water taken at his laboratory. B. Southworth made the figures of the CERN proton synchrotron and laboratory available. Ellen Cimpher patiently typed and retyped the manuscript with great good humor. R. Budnitz, H. P. Cantelow, J. Harris, and W. D. Hartsough read preliminary draft manuscripts and made several suggestions for improvements. The authors are also grateful to the hospitality of the National Laboratory for High Energy Physics, Oho-Machi, Japan, where the final version of this review was prepared.

This work was done with support from the U.S. Energy Research and Development Administration.

REFERENCES

1. Positron Electron Storage Ring Project, Report ERDA 1546, United States Energy Research and Development Administration, August 1976.
2. **Pigford, T. H.**, Environmental aspects of nuclear energy production, in *Annual Reviews of Nuclear Science*, Vol. 24, Annual Reviews, Palo Alto, 1974.
3. Report of Committee II on Permissible Dose for Internal Radiation, ICRP Publication 2, Internal Commission for Radiological Protection, Pergamon Press, Oxford, 1960.
4. **Gilbert, W. S., Keefe, D., McCaslin, J. B., Patterson, H. W., Smith, A. R., Stephens, L. D., Shaw, K. B., Stevenson, G. R., Thomas, R. H., Fortune, R. D., and Goebel, K.**, 1966 CERN-LRL-RHEL Shielding Experiment at the CERN Protonsynchrotron, Report UCRL-19741, Lawrence Berkeley Laboratory, Berkeley, 1968.

5. **Stapleton, G. B. and Thomas, R. H.,** Estimation of the induced radioactivity of the ground water system in the neighborhood of a proposed 300-GeV high-energy accelerator situated on a chalk site, *Health Phys.*, 23, 689, 1972.
6. **Martin, J. E. et al.,** quoted in Radioactivity from Fossil Fuel and Nuclear Power Plants, Paper SM-146/19, Symposium on Environmental Aspects of Nuclear Power Stations, New York, 1970.
7. Environmental Monitoring at Major ASAEC Contractor Sites, Calendar Year 1972, Report WASH-1259, USAEC, 1973.
8. Environmental Monitoring at Major USAEC Contractor Sites, Calendar Year 1973, Report WASH-125(73), USAEC, 1973.
9. Environmental Monitoring at Major Energy Research and Development Administration Contractor Sites, Calendar Year 1974, Report ERDA-54, USERDA, 1975.
10. **Hull, A. and Ash, J. A., Eds.,** 1974 Environmental Monitoring Report, Brookhaven National Laboratory, Report ERDA-54, USERDA, 1975, 397.
11. **Stevenson, G. R.,** The Radiation Environment of High-energy Proton-synchrotrons and Storage Rings, CERN-76-04, CERN Internal Report, presented at The Course of High-energy Dosimetry and Protection, Erice, Sicily, October 1975.
12. **Nelson, W. R. and Jenkins, T. M.,** Similarities between the radiation fields at different types of high-energy accelerators, *IEEE Trans. Nucl. Sci.*, NS-23, 135, 1976.
13. **Baker, S. J.,** Fermi National Accelerator Laboratory Environmental Monitoring Report for Calendar Year 1974, Report ERDA-54, USERDA, 1975, 561.
14. **Staebler, H. de,** Similarities of Shielding Problems at Electron and Proton Accelerators, Report CONF-651109, in Proc. of the Symp. on Accelerator Dosimetry, USAEC, Brookhaven, N.Y., 1965, 423.
15. **Jenkins, T. M.,** Accelerator boundary doses and skyshine, *Health Phys.*, 27, 1974, 251.
16. **McCaslin, J. B., Smith, A. R., Stephens, L. D., Thomas, R. H., Jenkins, T. M., Warren, G. J., and Baum, J.,** An Intercomparison of Dosimetry Techniques in Radiation Fields at Two High-energy Accelerators, Report LBL-5365, Lawrence Berkeley Laboratory, 1976.
17. **Thomas, R. H., Ed.,** The Environmental Surveillance Program of the Lawrence Berkeley Laboratory, Report LBL-4678, Lawrence Berkeley Laboratory, 1976.
18. **Prantl, F. A. and Baarli, J.,** Control of Radioactive Pollution in the Environment of the CERN Accelerators, Internal Report CERN 72-15, CERN Health Physics Group, 1972.
19. **Baarli, J. and Peetermans, A.,** Air Radioactivity from the CERN Accelerator Installation, Internal Report DI/HP/176, CERN Health Physics Group, 1974.
20. **Peetermans, A. and Baarli, J.,** Radioactive gas and aerosol production by the CERN high-energy accelerators and evaluation of their influences on environmental problems, in *Environmental Surveillance Around Nuclear Installations,* Vol. 1, International Atomic Energy Agency, Vienna, 1974, 433.
21. **Bonifas, A., Geroudet, J. M., Marchal, H., and Tuyn, J. W. N.,** On the Use of Thermoluminescent Dosimetry for Stray Radiation Monitoring on the CERN Site, Internal Report HP-74-138, CERN Health Physics Group, 1974.
22. **Grobon, G., Roubaud, G., and Tuyn, J. W. N.,** Stray Radiation Monitoring on the CERN Site during 1974, Internal Report HP-75-143, CERN Health Physics Group, 1975.
23. **Falk, R., Grobon, G., Renaud, C., Roubaud, G., and Tuyn, J. W. N.,** Environmental Radiation on the CERN Site during 1975, Internal Report HP-76-151, CERN Health Physics Group, 1976.
24. **Tuyn, J. W. N.,** Stray radiation monitoring around the CERN high-energy proton accelerators, Internal Report DI/HP/191, CERN Health Physics Group, 1975.
25. **Thomas, R. H.,** Neutron dosimetry at high-energy particle accelerators — a review, *Proc. IAEA Symp. on Neutron Monitoring,* Vol. 1, International Atomic Energy Agency, Vienna, 1972, 327.
26. **Lindenbaum, S. J.,** Proceedings of the Conference on Shielding of High-energy Accelerators, Report TID-7545, USAEC, New York, 1957, 28.
27. **Rindi, A. and Thomas, R. H.,** Skyshine, a paper tiger?, *Part. Accel.*, 7, 23, 1975.
28. **Ollendorf, W.,** A Study of Radiation Levels at the CERN Site, Internal Report DI/HP/66, CERN, 1964.
29. **Komochkov, M. M.,** The Dubna synchrophasotron, in *Engineering Compendium on Radiation Shielding,* Jaeger, R. G., Ed., Springer-Verlag, Berlin, 1970, 171.
30. **Distenfeld, C. and Colvett, R. D.,** Skyshine considerations for accelerator shielding design, *Nucl. Sci. Eng.*, 26, 117, 1966.
31. **Rindi, A. and Baarli, J.,** Scattered Radiation at Large Distances for the CERN 600 MeV Synchrocyclotron, Internal Report DI/HP/19, CERN, 1963.
32. **Bathow, G., Clausen, V., Freytag, E., and Tesch, K.,** Skyshine-Messungen und ihr Vergleich mit Abschätzungen aus der diffusionstheorie. *Nukleoni.*, 9, 14, 1967.
33. **Thomas, R. H., Shaw, K. B., Simpson, P. W., and MacEwan, J. E.,** Neutron Surveys around the Rutherford Laboratory 50-MeV Proton Linear Accelerator, Internal Report NIRL/M/30, Rutherford Laboratory, Chilton, England, 1962.
34. **Simpson, P. W. and Laws, D.,** Internal Report, Addendum to NIRL/M/30, Rutherford Laboratory, Chilton, England, 1962.
35. **Nakamura, T., Kawabata, H., Hayashi, K., Shin, K., Sugai, I., Hasegawa, T., and Ishizaki, Y.,** Skyshine of neutrons and photons from the INS FM-cyclotron, *Inst. Nucl. Study Univ. Tokyo Rep.*, 43, 1975.

36. **Cowan, F. P.,** A preliminary report on health physics problems at the Brookhaven Alternator Gradient Synchrotron, in *Premier Colloque International sur le Protection Aupres des Grands Accelerateurs,* Presses Universitaire de France, Paris, 1962, 143.
37. **Baarli, J. and Höfert, M.,** Some preliminary investigations of muons to the stray radiation level around the CERN 28 GeV protonsynchrotron, Proc. Third Intl. Congress of IRPA, Report CONF-730907, USAEC, 1973, 841.
38. **Stephens, L. D., Thomas, R. H., and Thomas, S. B.,** Population exposure from high-energy accelerators, *Health Phys.*, 29, 853, 1975.
39. **Stephens, L. D., Thomas, R. H., and Thomas, S. B.,** A model for estimating population exposures due to the operation of high-energy accelerators at the Lawrence Berkeley Laboratory, *Health Phys.*, 30, 404, 1976.
40. Implications of Commission Recommendations that Doses Be Kept as Low as Readily Achievable, International Commission on Radiological Protection, ICRP Publication 22, Pergamon Press, Oxford, 1973.
41. **Busick, D.,** Stanford Linear Accelerator Center, private communication, 1976.
42. **Busick, D.,** Environmental monitoring report, 1975, Stanford Linear Accelerator Center Publication, 194, 1976.
43. **Tuyn, J. W. N.,** CERN Health Physics Group, private communication, 1976.
44. **Hull, A. P. and Ash, J. A.,** 1975 Environmental Monitoring Report, Internal Report BNL 21320, Brookhaven National Laboratory, Brookhaven, 1976.
45. **Baker, S. I.,** Environmental Monitoring Report — Calendar Year 1975, Fermi National Accelerator Laboratory Report, Batavia, Ill., 1976.
46. **de Planque Burke, G.,** Variations in Natural Environmental Gamma Radiation and its Effect on the Interpretability of TLD Measurements Made Near Nuclear Facilities, Report HASL-287, Health and Safety Laboratory, New York, 1974.
47. **de Planque Burke, G.,** A model for estimating variations in terrestrial radiation exposures based on soil-water balance, in *Second Workshop on the Natural Radiation Environment,* Lowder, Wayne M., Ed., Health and Safety Laboratory Report HASL-287, 1974.
48. **Moore, W. H.,** Source of High-energy Particles from an Internal Target in the AGS, Internal Report AGSCD-62, Brookhaven Laboratory, Long Island, N.Y., 1966.
49. **Swanson, W.,** Stanford Linear Accelerator Center, private communication, 1976.
50. **Thomas, R. H.,** Possible contamination of ground water system by high-energy accelerators, in *Proc. of Fifth Annual Health Physics Society,* Mid-Year Topical Symposium on the Health Physics Aspects on Nuclear Facility Siting, Idaho Falls, 1970, 93.
51. **Patterson, H. W. and Thomas, R. H.,** Induced radioactivity of accelerators, *Accelerator Health Physics,* Academic Press, New York, 1973, ch. 7.
52. **Rose, B.,** Radioactivity of Synchrocyclotron Cooling Water, Internal Report AERE NP/R 2768, Atomic Energy Research Establishment, Harwell, England, 1958.
53. **Distenfeld, C.,** A Proposal for Increasing the Intensity of the AGS at the Brookhaven National Laboratory, Internal Report BNL-7956, Brookhaven National Laboratory, 1964.
54. **Stapleton, G. B. and Thomas, R. H.,** Radioassay of Irradiated Water Samples at Nimrod, Internal Note RP/PN/45, Rutherford Laboratory, Long Island, N.Y., 1967.
55. **Nelson, W. R.,** Radioactive Ground-water Produced in the Vicinity of Beam Dumps, Internal Note SLAC-TN-65-16, Stanford Linear Accelerator Center, Stanford, 1965.
56. **Middlekoop, W. C.,** Remarks about Ground Water Activation by a 300 GeV Proton Synchrotron, Internal Report ISR/INT BT/66-3, CERN, 1966.
57. **Rindi, A.,** Induced Radioactivity in the Cooling Waters of the CERN 300 GeV SPS, Internal Report Lab II-RA/Note/72-71, CERN, 1972.
58. **Stapleton, G. B. and Thomas, R. H.,** The production of ^{7}Be by 7 GeV proton interactions with oxygen, *Nucl. Phys. A*, 175, 124, 1971.
59. **Blythe, H. J.,** Some field trials on ground disposal by the industrial chemical group, Internal Report — AERE, GDF/P2, AERE, Harwell, England, undated.
60. **Komochkov, M. and Teterev, Yu.,** Activation of Water Cooling the Synchrocyclotron Units, Report P16-6314, Joint Institute of Nuclear Research, Dubna, 1972.
61. **Borak, T. B.,** Measurement of Induced Radioactivity in Cooling Waters for the CERN PS and External Beam Magnets, Internal Report HP-72-112, CERN Health Physics Group, 1972.
62. **Hoyer, F.,** Induced Radioactivity in the Earth Shielding on Top of High-energy Particle Accelerators, Report 68-42, CERN, 1968.
63. **Borak, T. B., Awschalom, M., Fairman, W., Iwami, F., and Sedlet, J.,** The underground migration of radionuclides produced in soil near high-energy proton accelerators, *Health Phys.*, 23, 679, 1972.
64. **Bruninx, E.,** High-energy Nuclear Reaction Cross Sections, Internal Reports 61-1, 62-9, 64-17, CERN, 1961, 1962, 1964.
65. **Baker, S. I.,** Soil Activation Measurements at Fermi Laboratory, Internal Report, Fermi National Accelerator Laboratory, Batavia, Ill., 1975.
66. **Baker, S. I.,** Environmental Monitoring Report for Calendar Year 1975, Internal Report, Fermi National Accelerator Laboratory, 1976.
67. **Thomas, R. H.,** Radioactivity in earth induced by high-energy electrons, *Nucl. Instrum. Methods,* 102, 149, 1972.

68. **Nelson, W. R., Jenkins, T. M., McCall, R. C., and Cobb, J. K.,** Electro-induced cascade showers in copper and lead at 1 GeV, *Phys. Rev.*, 149, 201, 1966.
69. **Bathow, G., Freytag, E., and Tesch, K.,** Shielding measurements on 4.8 GeV Bremsstrahling, *Nucl. Instrum. Methods*, 33, 261, 1965.
70. **Bathow, G., Freytag, E., and Tesch, K.,** Measurements on 6.3 GeV electromagnetic cascade and cascade-produced neutrons, *Nucl. Phys.*, B2, 669, 1967.
71. **Bathow, G., Freytag, E., and Tesch, K.,** Shielding of high-energy electrons: the neutron and muon components, *Nucl. Instrum. Methods*, 51, 56, 1967.
72. **Coleman, F. J., Shaw, K. B., and Stevenson, G. R.,** Proceedings of the Second International Symposium Accelerator Dosimetry, Report CONF-69110, USAEC, Stanford, 1969.
73. **Coleman, F. J., Thomas, D. C., and Saxon, G.,** An Experiment to Determine Shielding Requirements for a Multi-GeV Electron Synchrotron Ring, Internal Report DNPL/P72, Daresbury Nuclear Physics Laboratory, Daresbury, England, 1971.
74. **Cohen, B. L.,** Environmental hazards in radioactive waste disposal, *Phys. Today*, 29, 9, 1976.
75. **Mawson, C. A.,** Consequence of radioactive disposal into the ground, in *Health Physics*, Vol. 2, Part I, Duhamel, A. M. F., Ed., Pergamon Press, Oxford, 1969.
76. **Stapleton, G. B. and Thomas, R. H.,** The effect of sorption on the Migration of ^{7}Be from a high-energy accelerator constructed on a chalk site, *Water Res.*, 7, 1259, 1973.
77. **Schroeder, M. C., Crocker, M. C., and Blank, M. R.,** Internal Report, Sandia Laboratory, Albequerque, N.M., 1968.
78. **Mellish, C. E.,** *Radiochim. Acta*, 2, 204, 1964.
79. **Haymond, H. R.,** *J. Chem. Phys.*, 18, 1085, 1950.
80. **Gile, J. D.,** *J. Chem. Phys.*, 19, 256, 1951.
81. **Russel, J. E. and Ryan, R. M.,** Radioactive gas production from the R.P.I. electron linear accelerator, *IEEE Trans. Nucl. Sci.*, NS-12, 3, 678, 1965.
82. **George, A. C., Breslin, A. J., Haskins, J. W., Jr., and Ryan, R.R.,** Evaluation of the Hazard from Radioactive Gas and Ozone at Linear Electron Accelerators, Proc. 1st Symp. Accelerator Radiation Dosimetry and Experience, CONF-651109, Brookhaven National Laboratory, Long Island, N.Y., 513, 1965.
83. **Awschalom, M., Larsen, F. L., and Sass, R. E.,** The Radiation Measurements Group at the Princeton, Pennsylvania 3 GeV Proton Synchrotron, Proc. 1st Symp. Accelerator Radiation Dosimetry and Experience, CONF-651109, Brookhaven National Laboratory, Long Island, N.Y., 1965, 57.
84. **Rindi, A. and Charalambus, S.,** Airborne radioactivity produced at high-energy accelerators, *Nucl. Instrum. Methods*, 47, 227, 1967.
85. **Shaw, K. B. and Thomas, R. H.,** Radiation problems associated with a high-energy extracted proton beam, *Health Phys.*, 13, 1127, 1967.
86. **Awschalom, M., Larsen, F. L., and Schimmerling, W.,** Activation of argon near a target irradiated by 3 GeV protons, *Health Phys.*, 14(4), 345, 1968.
87. **Hofert, M.,** Radiation hazard of induced radioactivity in air as produced by high energy accelerators, *Proc. Second Int. Conf. on Accelerator Dosimetry and Experience*, SLAC, Stanford, 1969, CONF-691101, 111.
88. **Vialettes, H.,** Gas and dust activation in the target room of the Saclay electron linac identification of the produced radioactive nuclei and determination of the rejected activities, *Proc. Second Int. Conf. on Accelerator Dosimetry and Experience*, Stanford Linear Accelerator Center, Stanford, 1969, CONF-691101, 121.
89. **Prantl, F. A. and Baarli, J.,** Control of Radioactive Pollution in the Environment of the CERN Accelerators, Report 72-15, CERN, 1972.
90. **Rindi, A.,** La radioactivite indicite dans l'air de l'accelerateur de protons de 300 GeV du CERN, Internal Report RA/72-5, CERN Lab II, 1972.
91. **Peetermans, A. and Baarli, J.,** Radioactive gas and aerosol production by the CERN high energy accelerators and evaluation of their influences on environmental problems, *Environmental Surveillance around Nuclear Installations*, Vol. I, IAEA, Vienna, 1974, 433.
92. International Commission on Radiological Protection, Recommendations of the International Commission on Radiologic Protection, ICRP Publication 6, Pergamon Press, Oxford, 1964.
93. **Yamaguchi, C.,** MPC calculations for the radionuclides produced during accelerator operation, *Health Phys.*, 29, 393, 1975.
94. **Charalambus, S. and Rindi, A.,** Aerosol and dust radioactivity in the halls of high-energy accelerators, *Nucl. Instrum. Methods*, 56, 125, 1967.
95. **Busick, D. and Warren, G. J.,** Operational health physics associated with induced radioactivity at the Stanford Linear Accelerator Center, *Proc. Second Int. Conf. on Accelerator Dosimetry*, Stanford Linear Accelerator Center, Stanford, CONF-691101, 1969, 139.
96. **Patterson, H. W., Low-Beer, A. D., and Sargent, T. W.,** Whole-body counting and bioassay determination of accelerator workers, *Health Phys.*, 17, 621, 1965.
97. Annual Progress Report, Massachusetts Institute of Technology, Cambridge, May 1965.
98. **Van Dilla, M. A. and Engelke, M. J.,** Zinc-65 in cyclotron workers, *Science*, 131, 830, 1960.
99. **Anderson, A. L. and Schmidt, C. T.,** ^{65}Zn Content in 90-inch Cyclotron Workers at Livermore, Hazards Control Progress Report No. 25, Livermore Lawrence Radiation Laboratory, Livermore, Cal., 1966.

100. **Sargent, T. W.**, Lawrence Radiation Laboratory, private communication, 1962.
101. **Warren, G. J., Busick, D. D., and McCall, R. C.**, Radioactivity produced and released from water at high energies, in *Proc. Second Int. Conf. in Accelerator Dosimetry,* Stanford Linear Accelerator Center, Stanford, 1969, CONF-691101, 99.
102. **de Staebler, H., Jenkins, T. M., and Nelson, W. R.**, Shielding and radiations, in *The Stanford Two-mile Accelerator,* Neal, R. B., Ed., Benjamin, New York, 1968, ch. 26.
103. **Cocconi, G.**, Evaluation of the fluxes of secondary particles produced in high-energy proton collisions, *Nucl. Phys.*, 28B, 341, 1971.
104. **Levine, G. S., Squier, D. M., Stapleton, G. B., Stevenson, G. S., Goebel, K., and Ranft, J.**, The angular dependence of dose and hadron yields from targets in 8 GeV/c and 24 GeV/c extracted proton beams, *Part. Accel.*, 3, 91, 1972.
105. **Thomas, R. H., Ed.**, Annual Environmental Monitoring Report of the Lawrence Berkeley Laboratory — 1975, Report LBL-4827, Lawrence Berkeley Laboratory, Berkeley, 1976.
106. **Bunch, D. F.**, Dose to various body organs from inhalation or ingestion of soluble radionuclides, IDO-12054, Idaho Falls, 1966.
107. **Lebedev, V. N., Lukanin, V. S., Sychev, B. S., and Usakov, S. I.**, Gosudarstvennyj Komitet po Ispol Zovaniyu Atommoj Ehnergii SSSR, IFVE-LRI-75-6, Surpukhov Inst. Fiziki Vysokikh Ehnergij, Surpukhov, 1975.
108. **Balukova, V. D., Lukanin, V. S., Sychev, B. S., and Ushakov, S. I.**, Radioactivity of the Water in the Shield of Accelerators, Soviet Atomic Energy Commission, 765.

TECHNICAL INFORMATION DEPARTMENT
LAWRENCE BERKELEY LABORATORY
UNIVERSITY OF CALIFORNIA
BERKELEY, CALIFORNIA 94720